

①

**AD-A277 704**



**NASA CONTRACTOR REPORT 187573**

**INTERLAMINAR FRACTURE CHARACTERIZATION: A CURRENT REVIEW**

**Roderick H. Martin**

Analytical Services and Materials, Inc.  
107 Research Drive  
Hampton, Virginia 23666

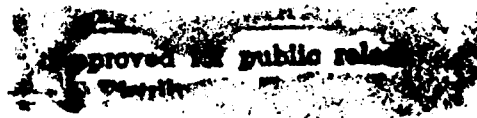
Contract NAS1-18599  
July 1991

**SDTIC**  
**ELECTE**  
**APR 01 1994**  
**S E D**

Abridged version of paper presented at  
2nd Japan International SAMPE Symposium  
Nippon Convention Center, Tokyo, Japan  
December 11-14, 1991

5178 **94-10080**

**NASA**  
National Aeronautics and  
Space Administration



**Langley Research Center**  
Hampton, Virginia 23665-5225

**94 4 1 149**

### SUMMARY

Interlaminar fracture characterization has been investigated for several years. Only now is it well enough understood for standardization organizations to attempt to write standard test methods. This paper gives a review of the current philosophies in characterizing interlaminar fracture. The paper covers all modes of interlaminar fracture for brittle and ductile composites. First, the mode I, double cantilever beam test (DCB) for measuring  $G_{Ic}$  and the end notched flexure test (ENF) for measuring  $G_{IIc}$  are discussed. These tests have undergone the most extensive research throughout the years and are furthest towards standardization. In addition, the mode II, end loaded split (ELS) specimen is discussed. Mixed mode fracture is also discussed and the recently developed mixed mode bending (MMB) test is detailed. Then, tests for evaluating mode III fracture toughness, including the split cantilever beam (SCB), are reviewed. Last, the work done on interlaminar fracture characterization in fatigue is reviewed.

### NOMENCLATURE

|          |  |
|----------|--|
| a        | delamination length                                |
| A        | constant in fatigue delamination growth expression |
| $A_1$    | slope of modified compliance expression            |
| b        | specimen width                                     |
| B        | exponent in fatigue delamination growth expression |
| c        | distance from load point to center of MMB fixture  |
| C        | specimen compliance, $\delta/P$                    |
| $C_0$    | constant in ENF compliance calibration             |
| $da/dN$  | delamination growth rate                           |
| $E_{11}$ | longitudinal modulus                               |
| $E_{22}$ | transverse modulus                                 |
| G        | strain energy release rate                         |
| $G_{13}$ | shear modulus                                      |
| $G_I$    | mode I strain energy release rate                  |
| $G_{Ic}$ | mode I interlaminar fracture toughness             |

|   |                         |
|---|-------------------------|
| <input checked="" type="checkbox"/><br><input type="checkbox"/> |                         |
| Unannounced<br>Justification                                    |                         |
| By _____  |                         |
| Distribution / _____  |                         |
| Availability Codes  |                         |
| Dist  | Avail and/or<br>Special |
| <b>A-1</b>  |                         |

|            |  |
|------------|--|
| $G_{Ith}$  | mode I fatigue threshold   |
| $G_{II}$   | mode II strain energy release rate                                   |
| $G_{IIc}$  | mode II interlaminar fracture toughness                              |
| $G_{III}$  | mode III strain energy release rate                                  |
| $G_{max}$  | maximum cyclic strain energy release rate                            |
| $h$        | beam half thickness  |
| $I$        | beam second moment of area   |
| $k$        | slope in ENF compliance expression                                   |
| $L$        | half span of ENF and MMB fixtures                                    |
| $m$        | constant in DCB compliance expression                                |
| $n$        | exponent in DCB compliance expression                                |
| $N$        | number of loading cycles   |
| $P$        | load   |
| $P_c$      | critical load  |
| $\delta$   | load point displacement  |
| $\delta_c$ | critical displacement  |
| $\Delta$   | correction to delamination length in modified beam theory expression |
| $\Delta G$ | cyclic amplitude of strain energy release rate                       |
| $\lambda$  | anisotropic constant for MMB specimen                                |
| $\chi$     | crack shear compliance   |

## INTRODUCTION

With the increased use of laminated fiber reinforced composite materials in primary aircraft structural components, the ability to understand and predict their failure modes becomes paramount. One of the most commonly observed damage modes in laminated composites is delamination, the separation of adjacent plies. Delamination is caused by interlaminar stresses arising from events such as low velocity impacts, by eccentricities in the load path, or by geometric and structural discontinuities such as holes, edges or ply drops. Although delamination may not cause total collapse of the load bearing properties of the component, it is usually a precursor to such an event. Therefore, knowledge of the composite's resistance to interlaminar fracture is useful not only

for product development and material screening, but a generic measurement of the interlaminar fracture toughness of the composite is useful for establishing design allowables for damage tolerance analyses of composite structures.

Several tests have been developed over the years to determine interlaminar fracture toughness, but until recently these tests have not been sufficiently refined to consider them for standardization. Since 1981 an American Society for Testing and Materials (ASTM) task group has been attempting to write standard test methods for interlaminar fracture tests. In 1989 the ASTM effort merged with that of the European Group on Fracture (now the European Structural Integrity Society) and the Japanese Industrial Standards Group, to write international test methods for these tests. Prior to these efforts, the lack of standardization has resulted in a wide range of interlaminar fracture toughness values being quoted for the same material [1]. This paper will attempt to review the current practices for characterizing interlaminar fracture toughness in terms of test configuration, test method and data reduction. For the interlaminar tension fracture (mode I), the double cantilever beam (DCB) test will be reviewed. For interlaminar sliding shear fracture (mode II), the end notched flexure (ENF) test will be reviewed. Also, the mode II, end loaded split (ELS) test is discussed. Mixed mode fracture is also reviewed and the recently developed mixed mode bending (MMB) test will be detailed. For interlaminar tearing shear, mode III, the

split cantilever beam (SCB) test will be discussed. Finally, the work done on interlaminar fracture in fatigue is reviewed.

## THE MODE I DOUBLE CANTILEVER BEAM TEST

### Specimen Configuration

The double cantilever beam specimen, shown in fig. 1, has been widely used to measure the mode I interlaminar fracture toughness,  $G_{Ic}$  of composites [1-12]. The DCB specimen is a laminate with a non-adhesive insert placed at the mid-plane at one end prior to curing, to simulate a delamination. Both  $0^\circ$  unidirectional [1-12] and multidirectional [13] lay-ups have been suggested. However, if  $90^\circ$  plies are used in a multidirectional lay-up these plies may be prone to cracking on loading, and additional delaminations may occur at these matrix cracks [14]. Also, because of the differences in Poisson's ratios between plies on either side of the delamination, interlaminar stresses arise at the edges, resulting in a non-uniform  $G$  distribution along the delamination front [15] and hence non-straight delamination growth. In addition, anticlastic bending which tends to increase the delamination front curvature [16,17] is more predominant in lay-ups that are not unidirectional. Hence, the unidirectional DCB is preferred.

Different width profiles from uniform width to tapered have been suggested for the DCB specimen [18]. The tapered width specimen was used to maintain a constant value of compliance as the delamination grew. Because of the extra work entailed in cutting the tapered width specimens the uniform width DCB specimen is more

often used. Various widths of DCB have been tested but typical widths range from 20-25mm. Also, various thicknesses (number of plies) of DCB have been used. Some references have shown that values of propagation interlaminar fracture toughness depend on specimen thickness; other references have shown a negligible dependence. In ref. 19 a 67% increase in thickness for IM6/PEEK specimens resulted in a 50% increase in toughness. But, only a 10% increase in toughness was noted with the same thickness increase in AS4/PEEK [20]. Reference 21 showed that there was little effect of specimen thickness on the initiation values of toughness for an AS4/PEEK specimen. Some thickness guidelines were given in refs. 22-24 to minimize the effects of geometric non-linearity in the DCB test. Typically, a 24 ply DCB is used to satisfactorily obtain  $G_{Ic}$  values without the need for geometric non-linearity corrections.

The method of load application in the DCB may also effect the data. Typically, loads are applied to the DCB via loading blocks or hinges adhesively bonded to the surface of the DCB. Load has also been applied via T-Tabs which can have a greater bonding area, allowing higher loads to be applied [24]. However, the height of the loading pin above the delamination surface causes a secondary geometric non-linearity upon loading. This secondary geometric non-linearity can also be accounted for in the data reduction schemes. However, if hinges or loading blocks can be sized so that the height of the loading pin above the delamination surface does not exceed 10mm, geometric non-linearity terms become negligible [24].

## Test Method

A uniform width unidirectional DCB specimen subjected to displacement controlled loading, usually experiences stable delamination growth [3,6]. This stable growth allows several values of mode I interlaminar fracture toughness to be determined along the specimen's length. However, for a unidirectional beam, fiber bridging occurs as the delamination progresses along the length of the beam [25,26]. Fiber bridging occurs to different degrees in different composite systems but is always present in standard unidirectional tape laminates. Fiber bridging increases the energy required to propagate the delamination further. Therefore, values of interlaminar fracture toughness,  $G_{Ic}$ , measured in the presence of fiber bridging may be artificially high and hence not a generic material property for the composite, but an artifact of the unidirectional DCB test. Only the first value of  $G_{Ic}$  obtained from delamination growth from the insert is unaffected by fiber bridging and can be considered a generic interlaminar fracture toughness [8,9,12]. However, during manufacture a resin pocket may form at the tip of the insert. The size of this resin pocket depends on the thickness of the insert and may also depend on the fiber stiffness and the viscosity of the resin in its liquid state. Therefore, a delamination growing from the insert tip must first pass through, or around, this resin pocket. This passage can result in artificially increased values of  $G_{Ic}$  at initiation. One possible means to circumvent the problems of a resin pocket is to

pre-crack the specimens, that is, to grow the delamination through the resin pocket either under tension or shear loading and then conduct the static test. However, if the pre-cracking is conducted in tension, fiber bridging will occur and the first value of  $G_{Ic}$  determined from the precrack will include the effects of fiber bridging. If the pre-crack is grown in shear, damage in the form of microcracks may occur ahead of the delamination front [27-29]. Hence, the first value of  $G_{Ic}$  from the pre-crack would be a measure of delamination through damaged material and would not be a generic material property.

Efforts have been made to quantify the effects of the size and type of the insert on initiation values of  $G_{Ic}$  [8,9,12]. The results for a glass/epoxy with four different insert thicknesses and a shear pre-crack are shown in fig. 2. The values of  $G_{Ic}$  appear to reach a minimum value for insert thicknesses less than  $75\mu\text{m}$ . References 8, 9 and 12 concluded that the thinnest insert possible should be used so that the size of the resin pocket that forms at the end of the insert will be as small as possible. Typically, the thinnest insert commercially available ranges between a 7 and  $13\mu\text{m}$  film. These thicknesses are approximately equivalent to one glass fiber diameter and are also the approximate thickness of the resin rich layer that lies between plies of different orientation. Hence,  $G_{Ic}$  values measured from the end of an insert of approximately these thicknesses should be representative of the fracture toughness of the composite.

There are several methods used to determine the loads and displacements corresponding to delamination initiation from the insert [12,20]. One method is to use the maximum value of load and the corresponding value of displacement from the load-displacement plot, point A in fig. 3. However, for a composite that experiences substantial fiber bridging, the load may continue to increase due to the increase of fiber bridging, and may never reach a maximum. Alternatively, the critical load and displacements for delamination initiation may be determined from the intersection of the load-displacement curve with a line corresponding to a 5% increase in initial compliance. This technique is analogous to that used in fracture testing of ductile homogeneous materials (ASTM E399-81). However, at the point of intersection, location B on fig. 3, delamination growth has typically already occurred. Therefore, the loads and displacements at location B should not be used to calculate  $G_{Ic}$  at initiation. An alternative method is to visually monitor the tip of the insert. When delamination growth is observed the load and displacement are noted, point C in fig. 3. Visual observation typically occurs at smaller loads and displacements than the previous two methods. The last alternative is to use the loads and displacements corresponding to a deviation from linearity of the initial loading slope, point D in fig. 3. For brittle composites, such as thermosets, the deviation from linearity occurs at the same moment delamination growth is observed visually [12], i.e. points C and D in fig. 3a would coincide. In

less brittle composites, such as those with thermoplastic matrices, the deviation from linearity occurs slightly before delamination growth is observed visually, fig. 3b. There are several possible reasons for the deviation from linearity prior to visual observation of delamination growth at the edges. The material could be deforming plastically prior to delamination initiation. However, the plastic zone ahead of the delamination front is usually very localized in a DCB [30] and is not likely to cause the large deviation from linearity observed in the load-displacement plots. Another possibility is that the delamination growth may be initiating in the center of the delamination front and is not yet visible at the edges [31]. Because the loads and displacements at deviation from linearity are lower than those from the other methods, these values yield the most conservative values of  $G_{Ic}$ . Also, this technique is simpler than the visual observation method because the tests may be run without the operator visually monitoring the end of the insert.

#### **Data Reduction**

The most commonly used data reduction technique for the DCB has been the Berry method [32]. With this method the compliance of the DCB is approximated by a power law,  $C = ma^n$ , where  $C$  is the compliance (load point displacement,  $\delta$ , divided by load,  $P$ ) and  $a$  is the delamination length. The fracture toughness is calculated by

$$G_{Ic} = \frac{n P_c \delta_c}{2 b a} \quad (1)$$

where  $\delta_c$  is the critical displacement,  $b$  is the width of the specimen and  $n$  is determined experimentally by a least squares plot of  $\log C$  versus  $\log a$ , fig. 4a. It is recognized that the calculated value of  $n$  may be influenced by fiber bridging. However, fiber bridging decreases the measured compliance with delamination length, thus reducing the value of  $n$ . Hence, ignoring the effects of fiber bridging yields conservative values of  $n$  and hence  $G_{Ic}$ .

The power law relationship of compliance to delamination length is relatively crude. An alternative method, known as the Modified Beam Theory [33] involves adjusting the measured delamination length by a value  $\Delta$ . Beam theory assumes that the cantilever beams are rigidly clamped at the delamination front, which may not be true. Therefore, the value of  $\Delta$  is used to account for any shear deformation or rotation at the delamination front. The fracture toughness is calculated by

$$G_{Ic} = \frac{3 P_c \delta_c}{2 b (a + |\Delta|)} \quad (2)$$

The value  $\Delta$  is determined experimentally by fitting a least squares curve to a plot of the cube root of the compliance,  $C^{1/3}$ , as a function of the delamination length. The value of  $\Delta$  is the value of  $a$  at  $C^{1/3}=0$ , fig. 4b. Again, the effects of fiber bridging are not included but have the effect of increasing  $|\Delta|$  and giving more

conservative values of  $G_{Ic}$  at initiation.

A third method known as the Modified Compliance Method [34] calculates the fracture toughness as

$$G_{Ic} = \frac{3 P_c^2 \left( \frac{\delta_c}{P_c} \right)^{2/3}}{2 A_1 b h} \quad (3)$$

where  $h$  is the half thickness of the beam and  $A_1$  is the slope of a least squares line fit to a plot of  $a/h$  as a function of the cube root of the compliance,  $C^{1/3}$ , fig. 4c. For this data reduction scheme, fiber bridging increases the value of  $A_1$  and hence reduces the value of  $G_{Ic}$  at initiation. All three methods give similar values of  $G_{Ic}$  with similar scatter and eq. 2 typically yields the most conservative values of the three.

## MODE II TESTS

### END NOTCHED FLEXURE TEST

#### Specimen Configuration

The end notched flexure specimen has been widely used to measure the mode II interlaminar sliding shear fracture toughness,  $G_{IIc}$ , of composites [28,29,35-37] and is shown schematically in fig. 5. The specimen configuration is similar to that of the DCB in that the lay-up is unidirectional, for the same reasons discussed for the DCB, and the sides are parallel. A non-adhesive insert is placed at the mid-plane at one end prior to curing. To apply the shear loading the specimen is loaded in three point bending. The loading fixture, shown in fig. 6, used rollers to

support the specimen and to allow it to rotate freely [1,28]. A restraining bar was included on the fixture at the end opposite the insert to prevent the specimen from shifting on the rollers during the test. Load point displacements were monitored via a displacement transducer (DCDT) mounted under the center of the specimen. The effects of specimen thickness and geometric non-linearity must be considered for the ENF specimens as they were for the DCB. If the beam is too thin then geometric non-linearity correction terms must be applied [38]. Typically, a 24-ply specimen is used to satisfactorily obtain  $G_{IIc}$  values without the need for geometric nonlinearity corrections.

#### **Test Method**

The ENF experiences unstable delamination growth even under displacement control for the majority of the useful length of the beam [35]. To obtain an R-curve, the specimen has to be tested once, moved in the fixture and re-tested. Since fiber bridging does not occur for a delamination grown in mode II, if any R-curve effect is observed it must be caused by another mechanism. As the delamination extends in shear, a large zone ahead of the delamination front is stressed [27]. This stress can cause damage ahead of the delamination front [29]. Hence, the ENF should not be pre-cracked in shear because any subsequent values of  $G_{IIc}$  would be toughness values corresponding to a delamination growing into damaged material and would not be a generic material property of the composite. A mode I pre-crack is also not recommended because

fiber bridging will occur. When the delamination subsequently tries to grow in shear, the bridged fibers must deform or break, thereby increasing the energy required to grow the delamination [12,36]. Studies of the effect of insert thickness and precracking on  $G_{IIC}$  initiation values were presented in refs. 12 and 39. The results for a glass/epoxy from ref. 12 are shown in fig. 7. Unlike the DCB, there was no apparent minimum value of  $G_{IIC}$  with decreased insert thickness for this glass/epoxy. Results from ref. 39 for an IM6/PEEK composite showed similar values of  $G_{IIC}$  at initiation from  $7\mu\text{m}$  and  $13\mu\text{m}$  inserts, indicating that an insert thickness between  $7\mu\text{m}$  and  $13\mu\text{m}$  may be appropriate for determining  $G_{IIC}$  values as in the DCB. In ref. 12 the  $G_{IIC}$  values at initiation from a shear or tensile pre-crack were higher than those from the thinner inserts. However, for other materials, the  $G_{IIC}$  values obtained from a precrack were lower than those obtained from a  $25\mu\text{m}$  thick insert [28,36].

Some attention has been given to determining the loads and displacements required to calculate the  $G_{IIC}$  values corresponding to delamination initiation [12,20,39]. Visual observation of delamination growth from the insert is difficult in the ENF because the delaminated surfaces are being pressed together and the delamination grows very rapidly. Therefore,  $G_{IIC}$  may be calculated using the loads and displacements corresponding to either the maximum load at which unstable delamination growth occurs, point A in fig. 8; the deviation from linearity of the load-displacement

curve, point B in fig. 8; or the intersection of the load-displacement curve with a line representing a 5% increase in initial compliance, point C in fig. 8. For brittle composites, even if the delamination is grown from the insert, there is a detectable non-linear portion to the load-displacement curve prior to unstable growth [12,39]. This non-linear portion may possibly be caused by the formation of microcracks or damage ahead of the delamination front, prior to coalescence of these cracks into delamination growth [29]. Also, the deviation from linearity may be caused by the delamination growth initiating at the center of the delamination front. The values of load and displacement at the deviation from linearity yield more conservative values of  $G_{IIC}$  than the maximum loads.

An alternative approach to conducting the ENF test was given in ref. 37. Here, the test is controlled by a clip gauge which measures the crack sliding displacement, CSD, fig. 9. By controlling the CSD, stable delamination growth is achieved and an R-curve can be obtained in one loading cycle.

#### **Data Reduction**

The most common method for reducing the ENF data is a beam theory expression for  $G_{IIC}$  with a correction for transverse shear [11,29,36]. This reduction scheme agreed well with predicted values from a 2-D finite element analysis [40]. Thus  $G_{IIC}$  may be calculated from

$$G_{IIc} = \frac{9 P_c \delta_c a^2}{2 b (2L^3 + 3a^3)} \left[ 1 + 0.2 \left( \frac{E_{11}}{G_{13}} \right) \left( \frac{h}{a} \right)^2 \right] \quad (4)$$

where L is the half span length and  $E_{11}$  and  $G_{13}$  are the longitudinal and shear moduli, respectively. An alternative data reduction technique involves determining the compliance as a function of delamination length. The ENF specimen is positioned in the loading fixture at different a/L lengths and loaded sufficiently to determine the compliance but not to propagate delamination. An expression for compliance is obtained from

$$C = C_o + ka^3 \quad (5)$$

where  $C_o$  and k are determined experimentally from a least squares fit to a plot of compliance versus  $a^3$ , and  $G_{IIc}$  is determined from

$$G_{IIc} = \frac{3 k a^2 P_c^2}{2 b} \quad (6)$$

For tests measuring CSD, as detailed in ref. 37,  $G_{IIc}$  values may be determined from

$$G_{IIc} = \frac{3 P_c^2 \chi}{8 b h} \quad (7)$$

where  $\chi$  is the crack shear compliance, CSD/P.

#### **END LOADED SPLIT TEST**

The end loaded split (ELS) test [41,42] has been used as a mode II test and has a similar configuration to the ENF. It is rigidly clamped at one end and loaded at the other as shown in

fig. 10. Because it is essential that the clamped end is rigid, the clamping fixture is usually fixed to the load frame. Hence, the fixture is not always readily transferrable from one load frame to another. The advantage of this specimen is that it has stable delamination growth for  $a/L > 0.55$ . Hence, any R-curve effect may be determined in one loading sequence.

#### MIXED MODE TESTING

Delaminations will not always occur in a pure mode fashion but may be a combination of all three modes. Therefore, a valid mixed mode failure criterion must be established. Most of the current research has focused on mixed mode I and II. Different types of specimens such as the cracked lap shear [7], the edge delamination test (EDT) [43,44], the Arcan [45], the asymmetric DCB [46], the mixed mode flexure [47], the variable mixed mode specimen [48] and others have been devised to give a combination of mode I and II. Some of the above tests require a finite element analysis to calculate the mode mix, and others, such as the asymmetric DCB, require a complicated loading mechanism.

Recently, a mixed mode bending (MMB) test, fig. 11, which has distinct advantages over the above mentioned mixed mode tests was developed [49] and modified [50]. By varying the position of the applied load point,  $c$ , the mixture of the modes can be altered. Thus, virtually any combination of modes I and II can be obtained from one specimen type. In addition, a closed form beam theory solution was developed to calculate the mode mix, thus avoiding the

use of finite element analysis. The mode I and II values for G can be calculated for  $c \geq L/3$  from

$$G_{Ic} = \frac{4 P_c^2 (3c - L)^2}{64 b L^2 E_{11} I} \left[ a^2 + \frac{2a}{\lambda} + \frac{1}{\lambda^2} + \frac{h^2 E_{11}}{10 G_{13}} \right] \quad (8)$$

$$G_{IIc} = \frac{3 P_c^2 (c + L)^2}{64 b L^2 E_{11} I} \left[ a^2 + \frac{h^2 E_{11}}{5 G_{13}} \right] \quad (9)$$

where

$$\lambda = \frac{1}{h} \left[ \frac{6 E_{22}}{E_{11}} \right]^{\frac{1}{4}} \quad (10)$$

Reference 50 gives details of the modifications made to the loading fixture to reduce geometric non-linearities. Results of ref. 50 indicate that for AS4/PEEK a suitable mixed mode I and II failure criterion may be

$$\left( \frac{G_I}{G_{Ic}} \right) + \left( \frac{G_{II}}{G_{IIc}} \right) = 1 \quad (11)$$

Further mixed mode tests (I and III; II and III; and I, II and III) need to be developed before eq. 11 could be extended to cover all three modes.

The edge delamination test (EDT) [43,44] has been used to conduct predominantly pure mode I tests as well as mixed mode tests. However, the values of G near the free edge are largely dependent on the amount of moisture the specimen has absorbed prior

to testing [51]. For this reason this specimen has not been widely accepted as an interlaminar fracture test. The EDT test has typically been used to quote edge delamination strength. But, these "strengths" will depend on the lay-up, stacking sequence and ply thickness of the test specimen. The EDT has one advantage over the MMB for studying environmental effects, such as exposure to temperature or fluids. Unlike the MMB, the delamination front in the EDT configuration in ref. 43 may be exposed to the environment. Therefore, the variation in fracture toughness caused by the environment may be directly measured [52,53].

#### MODE III TESTING

Little research has been conducted on mode III testing. Many analyses that are conducted on structures that are liable to delaminate are either 2-D [54], and hence have no mode III component or 3-D with uniaxial loading, causing a small to negligible mode III component [55]. However, some analyses show that the mode III component may be significant [56]. A mode III delamination test based on the rail shear test was developed in ref. 57. The rigidity of these specimens made compliance difficult to measure. In refs. 58 and 59 a split cantilever beam specimen (SCB) was developed and used to give mode III toughness values. This test was modified in ref. 60 and a 3-D finite element analysis was conducted to determine the modal distribution of  $G$  along the delamination front. The results, shown in fig. 12, indicated that there was a constant mode III distribution along the

delamination front. However, in addition there was a large mode II component which was zero in the center of the beam and significantly larger than the mode III component at the free edge. Examination of the failure surfaces from the experimental work in ref. 60, fig. 13, showed the failure surfaces along the delamination front were different at the edges than in the center of the beam. At the edges, shear hackles, indicative of mode II failure were observed, fig. 14. In the center of the beam, the failure surface was indicative of a mode III failure. Therefore, the split cantilever beam is not a pure mode III test. To date no adequate mode III test has been devised.

#### FATIGUE TESTING

The technique to characterize delamination fatigue has been studied by several authors and two methods currently exist; the delamination growth method and the delamination onset method. The DCB and ENF have been used to characterize fatigue delamination by monitoring the delamination growth per fatigue cycle,  $da/dN$  [1,61-66]. Expressions were given relating the applied cyclic strain energy release rate ( $G_{max}$  or  $\Delta G$ ) with  $da/dN$  in the form of a power law,  $da/dN = AG^B$  where A and B are constants that are determined experimentally. However, for composites, the values of the exponents, B, in these power laws were high, typically ranging from 3 to 10. Thus, any small deviation from the anticipated service load may lead to large errors in the predicted delamination growth rate using these power laws. This effect is shown

schematically in fig. 15. Thus,  $da/dN$  characterization may not be suitable for damage tolerance designs in composites.

An alternative design philosophy for composites utilizes the threshold value of strain energy release rate [67], such that if a flaw is known to exist, then the applied  $G$  must never exceed a threshold value, thus ensuring damage tolerance. The DCB and ENF tests have been used to obtain threshold values,  $G_{th}$ , in a manner similar to that used in metals. In the DCB, the delamination is allowed to grow under cyclic loading and the delamination growth rate is decreased until the delamination growth arrests [1,61,62]. However, this technique requires that the delamination be allowed to grow some distance before delamination arrest. As the delamination grows in fatigue, fiber bridging will occur as for the static tests. Therefore, when the delamination eventually arrests during the fatigue test, the measured  $G$  will include the effects of fiber bridging and will give artificially high values of  $G_{1th}$ .

An alternative method of obtaining threshold values using the DCB was demonstrated in refs. 1, 8, 12, 66 and 68. This method involved visually and electronically monitoring the onset of delamination growth at the end of the insert. If the delamination did not begin to grow before a specified number of cycles,  $N$ , then the applied  $G$  must be below the threshold value. By choosing a suitable value of  $N$  for the application, such as one million cycles, a desired value of  $G_{th}$  may be specified. If no delamination growth is observed after one million cycles, the

specimen is considered a runout as indicated by the arrows in fig. 16. That specimen is discarded and a new one tested at a higher load level. Because this method of determining thresholds uses only the initial delamination growth from the insert, the problems associated with delamination growth are eliminated. The use of delamination onset data may be further extended by testing several specimens at G values above the threshold value. Thus, it is possible to obtain a complete G-N curve for delamination growth onset, as shown in fig. 16.

Figure 17 shows the delamination growth plot for DCB specimens of the same glass/epoxy as used in fig. 16. Also plotted are the  $G_{1th}$  values at  $10^6$  cycles from fig. 16. If  $da/dN = 10^{-7}$  mm/cycle is considered to be delamination arrest, then the values of  $G_{1th}$  at  $10^6$  cycles can be seen to be significantly lower than the values of  $\Delta G$  at  $da/dN=10^{-7}$  mm/cycle. Therefore, using  $da/dN$  data to obtain a threshold strain energy release rate for damage tolerance designs could prove disastrous. However, G-N data of the type shown in fig. 16 may be used in life prediction methodologies such as detailed in refs. 53, 69-71. Using this methodology, each unique structural discontinuity in a composite structure must be analyzed to obtain a G distribution with delamination length. These calculated values of G are then compared to the G-N curves to predict delamination onset and growth in the structure.

## SUMMARY

This paper gave a review of the current techniques for characterizing interlaminar fracture. The mode I, double cantilever beam (DCB) test for measuring  $G_{Ic}$  and the end notched flexure (ENF) for measuring  $G_{IIc}$  were reviewed in terms of their configurations, testing methods, and data reduction. Also, the mode II end loaded split (ELS) test was discussed. Then, mixed mode delamination characterization was discussed and the mixed mode bending (MMB) test was detailed. Results of an analysis on the split cantilever beam (SCB) were given. This specimen has been proposed as a mode III test, but recent analysis has shown that this specimen delaminates in a combination of modes II and III. Therefore, to date no recommended mode III test is available. Lastly, techniques for characterizing interlaminar fracture by fatigue were reviewed. Two techniques for fatigue characterization exist: The delamination growth method and the delamination onset method. This paper reviewed the work done using both methods and details the advantages of the onset method versus the growth method.

## REFERENCES

1. Martin, R.H. and Murri, G.B., "Characterization of Mode I and Mode II Delamination Growth and Thresholds in AS4/PEEK Composites," Composite Materials: Testing and Design (Ninth Volume), ASTM STP 1059, S.P. Garbo, Ed., American Society for Testing and Materials, Philadelphia, 1990, pp. 251-270.

2. Wilkins, D.J., Eisenmann, J.R., Camin, R.A., Margolis, W.S., and Benson, R.A., "Characterizing Delamination Growth in Graphite/Epoxy," Damage in Composite Materials, ASTM STP 775, K.L. Reifsnider, Ed., American Society for Testing and Materials, Philadelphia, 1982, pp. 168-183.
3. Whitney, J.M., Browning, C.E., and Hoogsteden, W., "A Double Cantilever Beam Test for Characterizing Mode I Delamination of Composite Materials," Journal of Reinforced Plastics and Composites, Vol.1, October 1982, pp.297-313.
4. Carlile, D.R. and Leach, D.C., "Damage and Notch Sensitivity of Graphite/PEEK Composites," Proceedings of the 15th National SAMPE Technical Conference, October 1983, pp. 82-93.
5. de Charentenay, F.X., Harry, J.M., Prel, Y.J., and Benzeggagh, M.L., "Characterizing the Effect of Delamination Defect by Mode I Delamination Test," Effects of Defects in Composite Materials, ASTM STP 836, D.J. Wilkins, Ed., American Society for Testing and Materials, Philadelphia, 1984, pp. 84-103.
6. Keary, P.E., Ilcewicz, L.B., Shaar, C., and Trostle, J., "Mode I Interlaminar Fracture Toughness of Composite Materials Using Slender Double Cantilever Beam Specimens," Journal of Composite Materials, Vol.19, March 1985, pp. 154-177.
7. Ramkumar, R.L. and Whitcomb, J.D., "Characterization of Mode I and Mixed Mode Delamination Growth in T300/5208 Graphite/Epoxy," Delamination and Debonding of Materials, ASTM STP 876, W.S. Johnson, Ed., American Society for Testing and Materials, Philadelphia, 1985, pp. 315-335.
8. Martin, R.H., "Effect of Initial Delamination on  $G_{Ic}$  and  $G_{Ith}$  Values from Glass/Epoxy Double Cantilever Beam Tests," Proceedings of the American Society for Composites, Third Technical Conference, Seattle, Washington, September 1988, pp. 688-701.
9. Davies, P., Cantwell, W., and Kausch, H.H., "Measurement of Initiation Values of  $G_{Ic}$  in IM6/PEEK Composites," Composites Science and Technology, Vol.35, 1989, pp. 301-313.
10. Prel, Y.J., Davies, P., Benzeggagh, M.L., and de Charentenay, F., "Mode I and Mode II Delamination of Thermosetting and Thermoplastic Composites," Composite Materials: Fatigue and Fracture (Second Volume), ASTM STP 1012, P.A. Lagace, Ed., American Society for Testing and Materials, Philadelphia, 1989, pp. 251-269.

11. Mall, S., Yun, K.T., and Kochhar, N.K., "Characterization of Matrix Toughness Effect on Cyclic Delamination Growth in Graphite Fiber Composites," Composite Materials: Fatigue and Fracture (Second Volume), ASTM STP 1012, P.A. Lagace, Ed., American Society for Testing and Materials, Philadelphia, 1989, pp. 296-310.
12. Murri, G.B., and Martin, R.H., "Effect of Starter Delamination on Mode I and Mode II Fracture Toughness and Threshold Strain Energy Release Rates," Presented at the Fourth ASTM Symposium on Composite Materials: Fatigue and Fracture, Indianapolis, Indiana, May 6-7, 1991. Also published as NASA TM 104079, 1991.
13. Jordan, W.M., "The Toughness of Damaged or Imperfect Laminates," Proceedings of the American Society for Composites, Third Technical Conference, Seattle, WA, September 1988, pp. 495-502.
14. Wang, A.S.D and Crossman, F.W., "Initiation and Growth of Transverse Cracks and Edge Delamination in Composite Laminates Part 1. An Energy Method," Journal of Composite Materials Supplement, Vol. 14, 1980, pp. 71-87.
15. Salpekar, S.A. and O'Brien, T.K., "Combined Effect of Matrix Cracking and Stress-Free Edge on Delamination," Composite Materials: Fatigue and Fracture (3rd Volume) ASTM STP 1110, T.K. O'Brien, Ed., American Society for Testing and Materials, Philadelphia, 1991, pp. 000-000. Also published as NASA TM 102591, March 1990.
16. Crews, J.H. Jr., Shivakumar, K., and Raju, I.S., "Effects of Anticlastic Curvature on G Distributions for DCB Specimens," AIAA-89-1300, Proceedings of the 30th AIAA/ASME/ASCE/AHS/ASC Conference on Structures, Structural Dynamics and Materials, Mobile, Alabama, April 3-5, 1989, pp.1242-1249.
17. Davidson, B.D., "An Analytical Investigation of Delamination Front Curvature in Double Cantilever Beam Specimens," Journal of Composite Materials, Vol. 24, November 1990, pp. 1124-1137.
18. Kanninen, M.F., Popelar, C., and Gehlen, P.C., "Dynamic Analysis of Crack Propagation and Arrest in the Double Cantilever Beam Specimen," Fast Fracture and Crack Arrest, ASTM STP 627, G.T. Hahn and M.F. Kanninen, Eds., American Society for Testing and Materials, Philadelphia, 1977, pp. 19-38.

19. Davies, P., Cantwell, W., Moulin, C., and Kausch, H.H., "A Study of the Delamination Resistance of IM6/PEEK Composites," *Composites Science and Technology*, Vol. 36, No. 2, (1989), pp. 153-166.
20. Davies, P., "Round Robin Interlaminar Fracture Testing of Carbon Fibre Reinforced Epoxy and PEEK Composites," to be published in *Composites Science and Technology*, 1991.
21. Hojo, M., Aoki, T., and Tanaka, K., "Thickness Effect of DCB Specimen on Interlaminar Fracture Toughness of AS4/PEEK and T800/Epoxy Laminates," Presented at the Fourth ASTM Symposium on Composite Materials: Fatigue and Fracture, Indianapolis, Indiana, May 6-7, 1991.
22. Whitcomb, J.D., "A Simple Calculation of Strain Energy Release Rate for a Nonlinear Double Cantilever Beam," *Journal of Composites Technology and Research*, Vol.7, No.2, Summer 1985, pp. 64-66.
23. Williams, J.G., "Large Displacement and End Block Effects in the DCB Interlaminar Test in Modes I and II," *Journal of Composite Materials*, Vol.21, April 1987, pp. 330-347.
24. Naik, R.A., Crews, J.H. Jr., and Shivakumar, K.N., "Effects of T-Tabs and Large Deflections in DCB Specimen Tests," Composite Materials: Fatigue and Fracture (3rd Volume) ASTM STP 1110, T.K. O'Brien, Ed., American Society for Testing and Materials, Philadelphia, 1991, pp. 000-000. Also published as NASA TM 101677, November 1989.
25. Russell, A.J., "Factors Affecting the Opening Mode Delamination of Graphite/Epoxy Laminates," Defence Research Establishment Pacific (DREP), Canada, Materials Report 82-Q, December 1982.
26. Johnson, W.S. and Mangalgiri, P.D., "Investigation of Fiber Bridging in Double Cantilever Beam Specimens," *Journal of Composites Technology and Research*, Vol.9, No.1, Spring 1987, pp. 10-13.
27. Corletto, C., Bradley, W., and Henriksen, M. "Correspondence Between Stress Fields and Damage Zones Ahead of the Crack Tip of Composites Under Mode I and Mode II Delaminations," *Proceedings of the 6th ICCM and 2nd ECCM Conference*, Elsevier Applied Science, London, Vol.3, July 1987, pp. 3.378-3.387.

28. Murri, G.B. and O'Brien, T.K., "Interlaminar  $G_{IIc}$  Evaluation of Toughened Resin Matrix Composites Using the End-Notched Flexure Test," AIAA-85-0647, Proceedings of the 26th AIAA/ASME/ASCE/AHS Conference on Structures, Structural Dynamics and Materials, Orlando, Florida, April 1985, pp. 197-202.
29. O'Brien, T.K., Murri, G.B., and Salpekar, S.A., "Interlaminar Shear Fracture Toughness and Fatigue Thresholds for Composite Materials," Composite Materials: Fatigue and Fracture (Second Volume), ASTM STP 1012, P.A. Lagace, Ed., American Society for Testing and Materials, Philadelphia, 1989, pp. 222-250.
30. Walter, K.F.R., Carlsson, L.A., Smiley, A.J., and Gillespie, J.W., Jr., "Mechanisms for Rate Effects on Interlaminar Fracture Toughness of Carbon/Epoxy and Carbon/PEEK Composites," Journal of Materials Science, 24 (1989) pp. 3387-3398.
31. de Kalbermätten, T., Jaggi, R., and Fluëler, P., "Interlaminares Bruchverhalten von CFK-Epoxy/PEEK- Laminaten in Mode I an DCB-Proben," EMPA Report No. 116'598/ZEP, Swiss Federal Laboratories for Materials Testing and Research, Dübendorf, Switzerland, September 1990.
32. Berry, J.P., "Determination of Fracture Energies by the Cleavage Technique," Journal of Applied Physics, Vol.34, No. 1, January 1963, pp. 62-68.
33. Hashemi, S., Kinloch, A.J., and Williams, J.G., "Corrections Needed in Double Cantilever Beam Tests for Assessing the Interlaminar Failure of Fibre-composites," J. of Materials Science Letters, Vol. 8, 1989, pp. 125-129.
34. Chang, W.-T., Kimpara, I., Kageyama, K., and Ohsawa, I., "New Data Reduction Schemes for the DCB and ENF Tests of Fracture Resistant Composites," Proceedings of the Fourth European Conference on Composite Materials, Stuttgart, F.R.G., September 1990, pp. 503-508.
35. Russell, A.J. and Street, K.N., "The Effect of Matrix Toughness on Delamination: Static and Fatigue Fracture Under Mode II Shear Loading of Graphite Fiber Composites," Toughened Composites, ASTM STP 937, N.J. Johnston, Ed., American Society for Testing and Materials, Philadelphia, 1987, pp. 275-294.

36. Russell, A.J., "Initiation of Mode II Delamination in Toughened Composites," Composite Materials: Fatigue and Fracture (3rd Volume), ASTM STP 1110, T.K. O'Brien, Ed., American Society for Testing and Materials, Philadelphia, 1991, pp. 000-000.
37. Kageyama, K., Kikuchi, M., and Yanagisawa, N., "A Stabilized End Notched Flexure Test," Composite Materials: Fatigue and Fracture (3rd Volume), ASTM STP 1110, T.K. O'Brien, Ed., American Society for Testing and Materials, Philadelphia, 1991, pp. 000-000.
38. Williams, J.G., "Large Displacement and End Block Effects in the DCB Interlaminar Test in Modes I and II," Journal of Composite Materials, Vol. 21, April 1987, pp. 330-347.
39. Davies, P., Cantwell, W.J., and Kausch, H.H., "Delamination From Thin Starter Films in Carbon Fibre/PEEK Composites," Journal of Materials Science Letters, Vol. 9, Nov. 1990, pp. 1349-1350.
40. Salpekar, S.A., Raju, I.S., and O'Brien, T.K., "Strain Energy Release Rate Analysis of the End-Notched Flexure Specimen Using the Finite Element Method," Journal of Composites Technology & Research, Vol. 10, No. 4, Winter 1988, pp. 133-139.
41. Hashemi, S., Kinloch, A.J., and Williams, J.G., "The Analysis of Interlaminar Fracture in Uniaxial Fibre-Polymer Composites," Proceedings of the Royal Society of London, A 427, 1990, pp. 173-199.
42. Corletto, C.R., "Mode II Delamination Fracture Toughness of Unidirectional Graphite/Epoxy Composites," MSc Thesis, Texas A&M University, Texas, 1986.
43. O'Brien, T.K., Johnston, N.J., Morris, D.H., and Simmonds, R.A., "Determination of Interlaminar Fracture Toughness and Fracture Mode Dependence of Composites Using the Edge Delamination Test," Proceedings of the International Conference on Testing, Evaluation and Quality Control of Composites, University of Surrey, Guildford, England, September, 1983, pp. 223-232.
44. Whitney, J.M. and Knight, M., "A Modified Free-Edge Delamination Specimen," Delamination and Debonding of Materials, ASTM STP 876, W.S. Johnson, Ed., American Society for Testing and Materials, Philadelphia, 1985, pp. 298-314.

45. Arcan, M., Hashin, Z., and Voloshin, A., "A Method to Produce Uniform Plane-Stress States with Applications to Fiber-Reinforced Materials," *Experimental Mechanics*, Vol. 8, April 1978, pp. 141-146.
46. Bradley, W.L. and Cohen, R.N., "Matrix Deformation and Fracture in Graphite-Reinforced Epoxies," Delamination and Debonding of Materials, ASTM STP 876, W.S. Johnson, Ed., American Society for Testing and Materials, Philadelphia, 1985, pp. 389-410.
47. Russell, A.J. and Street, K.N., "Moisture and Temperature Effects on the Mixed Mode Delamination Fracture of Unidirectional Graphite/Epoxy," Delamination and Debonding of Materials, ASTM STP 876, W.S. Johnson, Ed., American Society for Testing and Materials, Philadelphia, 1985, pp. 349-370.
48. Hashemi, S., Kinloch, A.J., and Williams, J.G., "Interlaminar Fracture of Composite Materials," *Proceedings of the 6th ICCM and 2nd ECCM Conference*, Elsevier Applied Science, London, Vol. 3, July 1987, pp. 3.254-3.264
49. Reeder, J.R. and Crews, J.H., Jr., "Mixed-Mode Bending Method for Delamination Testing," *AIAA Journal*, Vol. 28, No. 7, July 1990, pp. 1270-1276.
50. Reeder, J.R., and Crews, J.H., Jr., "Nonlinear Analysis and Re-Design of the Mixed Mode Bending Delamination Test," To be presented at the ICCM VIII, Honolulu, Hawaii, July 1991. Also published as NASA TM 102777, January 1991.
51. O'Brien, T.K., Raju, I.S., and Garber, D.P., "Residual Thermal and Moisture Influences on the Strain Energy Release Rate Analysis of Edge Delamination," *Journal of Composites Technology & Research*, Vol. 8, No. 2, Summer 1986, pp. 37-47
52. Hooper, S.J., Toubia, R.F., and Subramanian, R., "The Effects of Moisture Absorption on Edge Delamination, Part 2: An Experimental Study of Jet Fuel Absorption on Graphite/Epoxy," Composite Materials: Fatigue and Fracture (3rd Volume), ASTM STP 1110, T.K. O'Brien, Ed., American Society for Testing and Materials, Philadelphia, 1991, pp. 000-000.
53. Martin, R.H. "Delamination Onset and Accumulation in Polymeric Composite Laminates Under Cyclic Thermal and Mechanical Loads," to be presented at the ASTM Symposium on High Temperature and Environmental Effects on Polymeric Composites, San Diego, California, October 15-16, 1991.

54. Salpekar, S.A., Raju I.S., and O'Brien T.K., "Strain Energy Release Rate Analysis of Delamination in a Tapered Laminate Subjected to Tension Load," Proceedings of the American Society for Composites, Third Technical Conference, Seattle, WA, September 1988, pp. 642-654.
55. Whitcomb, J.D, "Mechanics of Instability-Related Delamination Growth," Composite Materials: Testing and Design (Ninth Volume), ASTM STP 1059, S.P. Garbo, Ed., American Society for Testing and Materials, Philadelphia, 1990, pp. 215-230.
56. O'Brien, T.K. and Raju, I.S., " Strain Energy Release Rate Analysis of Delamination Around an Open Hole in a Composite Laminate," AIAA-84-0961, Proceedings of the 25th AIAA/ASME/ASCE/AHS Structures, Structural Dynamics, and Materials Conference, Palm Springs, CA, May 1984.
57. Becht, G., and Gillespie, J.W., Jr., "Design and Analysis of a Mode III Interlaminar Fracture Specimen," Proceedings of the American Society for Composites, Second Technical Conference, Newark, Delaware, September 1987, pp. 9-18.
58. Donaldson, S.L., "Interlaminar Fracture Due to Tearing (Mode III), 6th ICCM & 2nd ECCM Conference Proceedings, Elsevier Applied Science, London, Vol. 3, July 1987, pp. 3.274-3.283.
59. Lingg, C.L., Mall, S., and Donaldson, S.L., "Loading Rate Effect on Mode III Delamination Fracture Toughness of Graphite/Epoxy," Proceedings of the American Society for Composites, Fourth Technical Conference, Blacksburg, Virginia, October 1989, pp. 267-276.
60. Martin, R.H., "Evaluation of the Split Cantilever Beam for Mode III Delamination Testing," Composite Materials: Fatigue and Fracture (3rd Volume), ASTM STP 1110, T.K. O'Brien, Ed., American Society for Testing and Materials, Philadelphia, 1991, pp. 000-000. Also published as NASA TM 101562, March 1989.
61. Bathias, C. and Laksimi, A., "Delamination Threshold and Loading Effect in Fiberglass Epoxy Composite," Delamination and Debonding of Materials, ASTM STP 876, W.S. Johnson, Ed., American Society for Testing and Materials, Philadelphia, 1985, pp. 217-237.
62. Hojo, M., Tanaka, K., Gustafson, C.G., and Hayashi, R., "Effect of Stress Ratio on Near-threshold Propagation of Delamination Fatigue Cracks in Unidirectional CFRP," Composites Science and Technology, 29, 1987, pp. 273-292.

63. Russell, A.J. and Street K.N., "A Constant AG Test for Measuring Mode I Interlaminar Fatigue Crack Growth Rates," Composite Materials: Testing and Design (Eighth Conference), ASTM STP 972, J.D. Whitcomb, Ed., American Society for Testing and Materials, Philadelphia, 1988, pp. 259-277.
64. Hojo, M., Tanaka, K., Gustafson, C.G., and Hayashi, R., "Propagation of Delamination Fatigue Cracks in CFRP in Water," JSME International Journal, Series I, Vol.32, No. 2, 1989, pp. 292-299.
65. Russell, A.J. and Street, K.N., "Predicting Interlaminar Fatigue Crack Growth Rates in Compressively Loaded Laminates," Composite Materials: Fatigue and Fracture (Second Volume), ASTM STP 1012, P.A. Lagace, Ed., American Society for Testing and Materials, Philadelphia, 1989, pp. 162-178.
66. Martin, R.H., "Characterizing Mode I Fatigue Delamination of Composite Materials," Proceedings of the Mechanics Computing in 1990 and Beyond Conference, Columbus, Ohio, May 19-22, 1991, Vol. 2, pp. 943-948.
67. O'Brien T.K., "Towards a Damage Tolerance Philosophy for Composites Materials and Structures," Composite Materials: Testing and Design (Ninth Volume), ASTM STP 1059, S.P. Garbo, Ed., American Society for Testing and Materials, Philadelphia, 1990, pp. 7-33.
68. Davies P., Cantwell, W.J., Jar, P., Y., Richard, H., Neville, D.J., and Kausch, H.H., "Cooling Rate Effects in Carbon Fibre/PEEK Composites," Composite Materials: Fatigue and Fracture (3rd Volume), ASTM STP 1110, T.K. O'Brien, Ed., American Society for Testing and Materials, Philadelphia, 1991, pp. 000-000.
69. O'Brien, T.K., Rigamonti, M., and Zanotti, C., "Tension Fatigue Analysis and Life Prediction for Composite Laminates," International Journal of Fatigue, 11, No. 6, 1989, pp. 379-393.
70. Murri, G.B., Salpekar, S.A, and O'Brien, T.K., "Fatigue Delamination Onset Prediction in Tapered Composite Laminates," Composite Materials: Fatigue and Fracture (3rd Volume), ASTM STP 1110, T.K. O'Brien, Ed., American Society for Testing and Materials, Philadelphia, 1991, pp. 000-000. Also published as NASA TM 101673, December 1989.

71. Martin, R.H., and Jackson, W.C., "Damage Prediction in Cross-plyed Curved Laminates," Presented at the Fourth ASTM Symposium on Composite Materials: Fatigue and Fracture, Indianapolis, Indiana, May 6-7, 1991. Also published as NASA TM 104089, 1991.

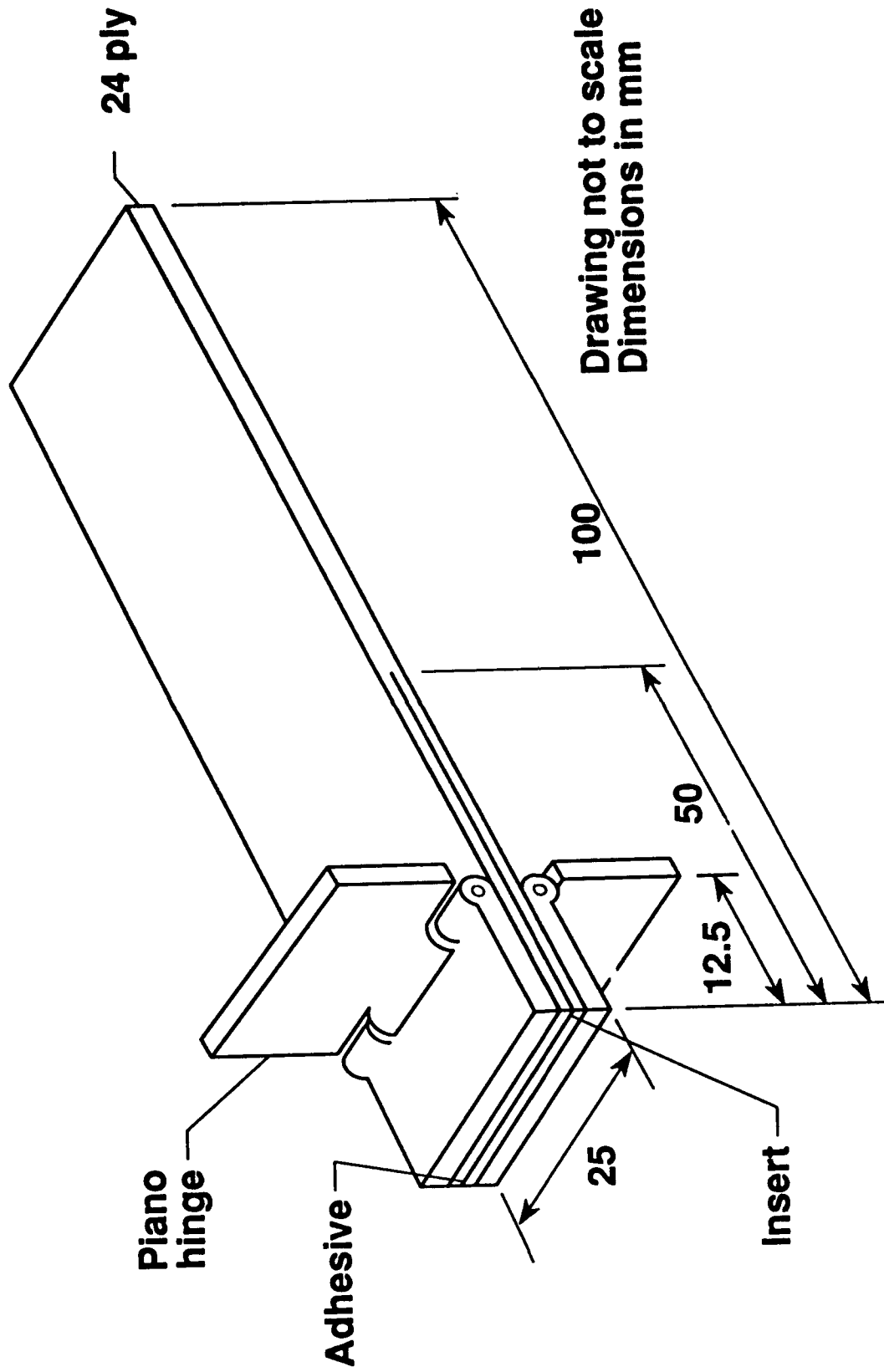


Fig. 1. - Double cantilever beam specimen.

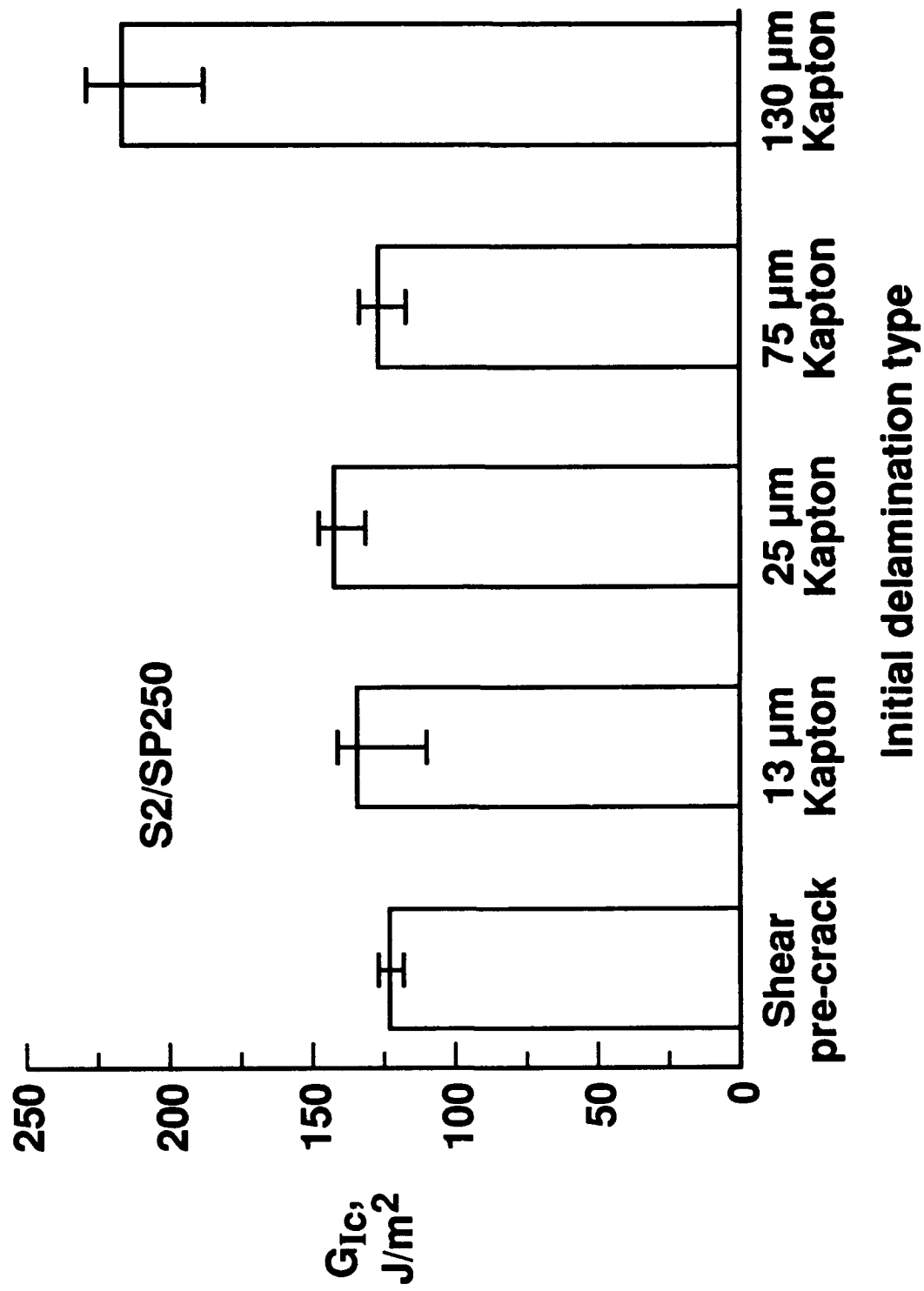


Fig. 2. - Effect of initial delamination on  $G_{IC}$  at initiation.

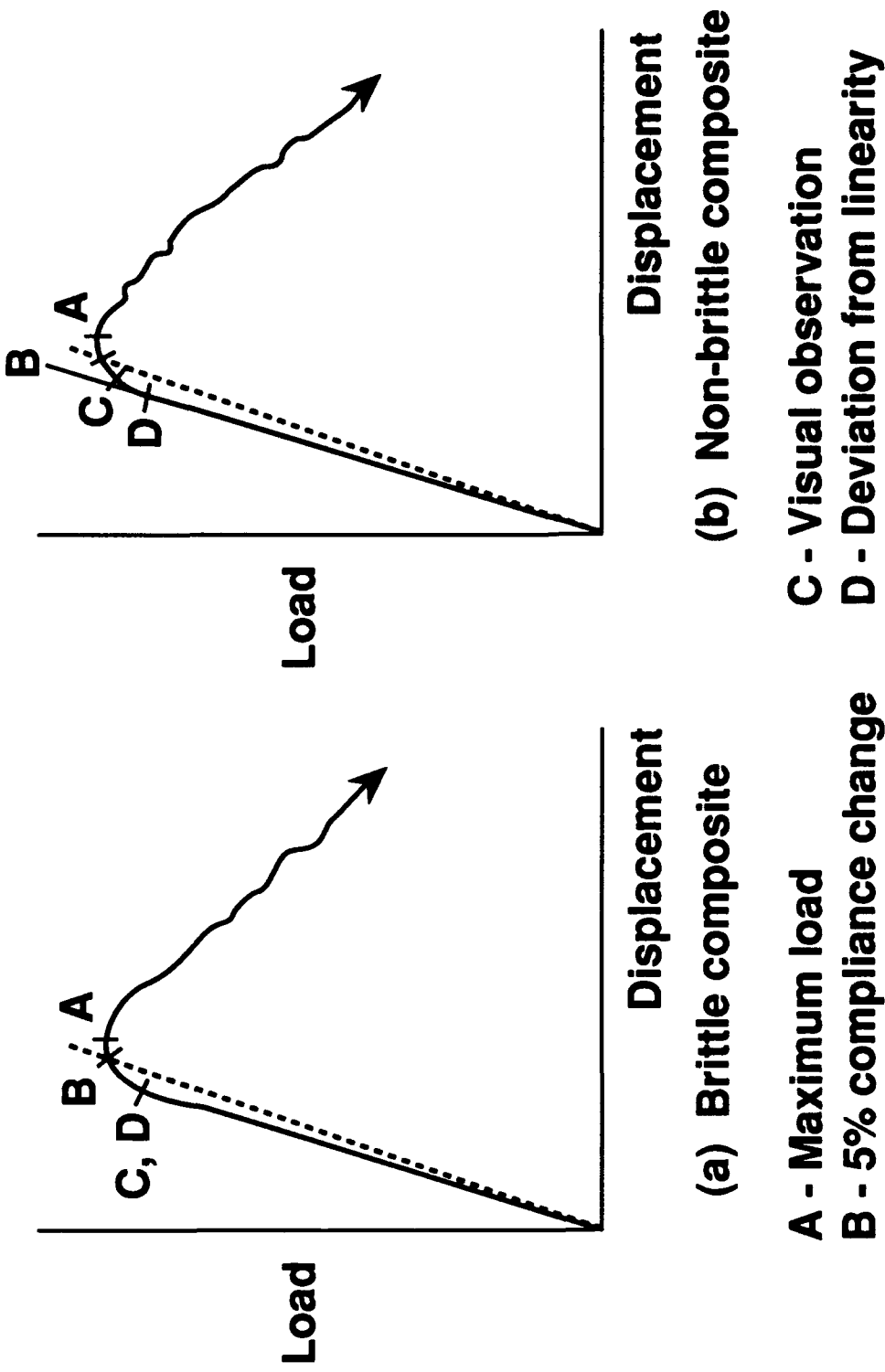
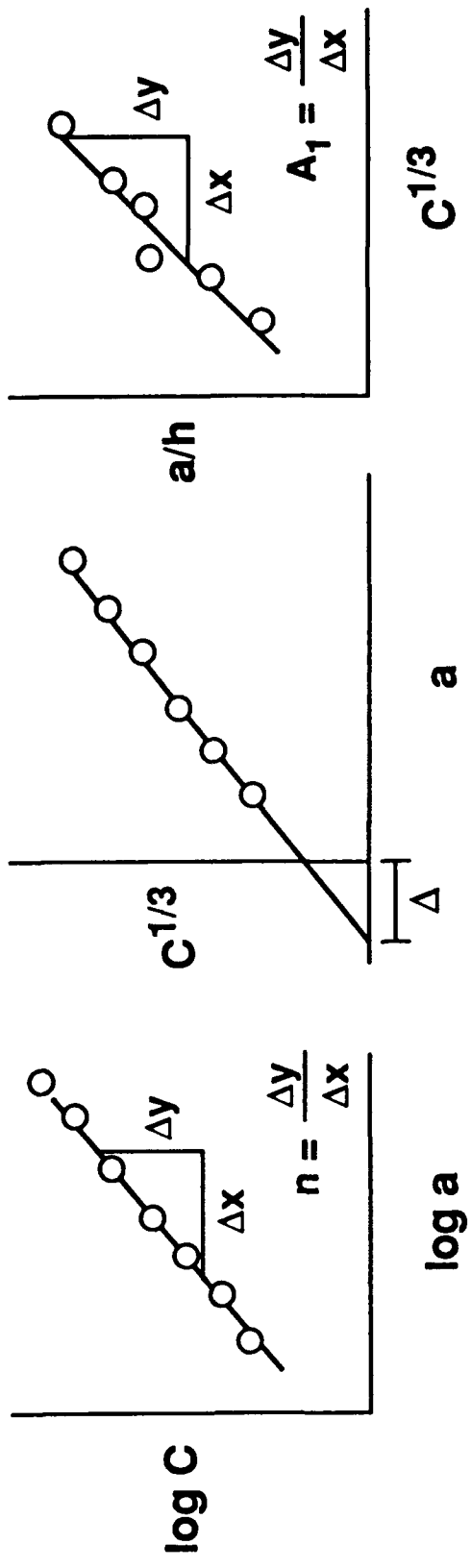


Fig. 3. - Schematic of load-displacement plots for DCB specimen.



a) Berry Method      b) Modified Beam Theory      c) Modified Compliance Calibration Method

Fig. 4. - Experimental data fitting to obtain constants for  $G_{Ic}$  determination.



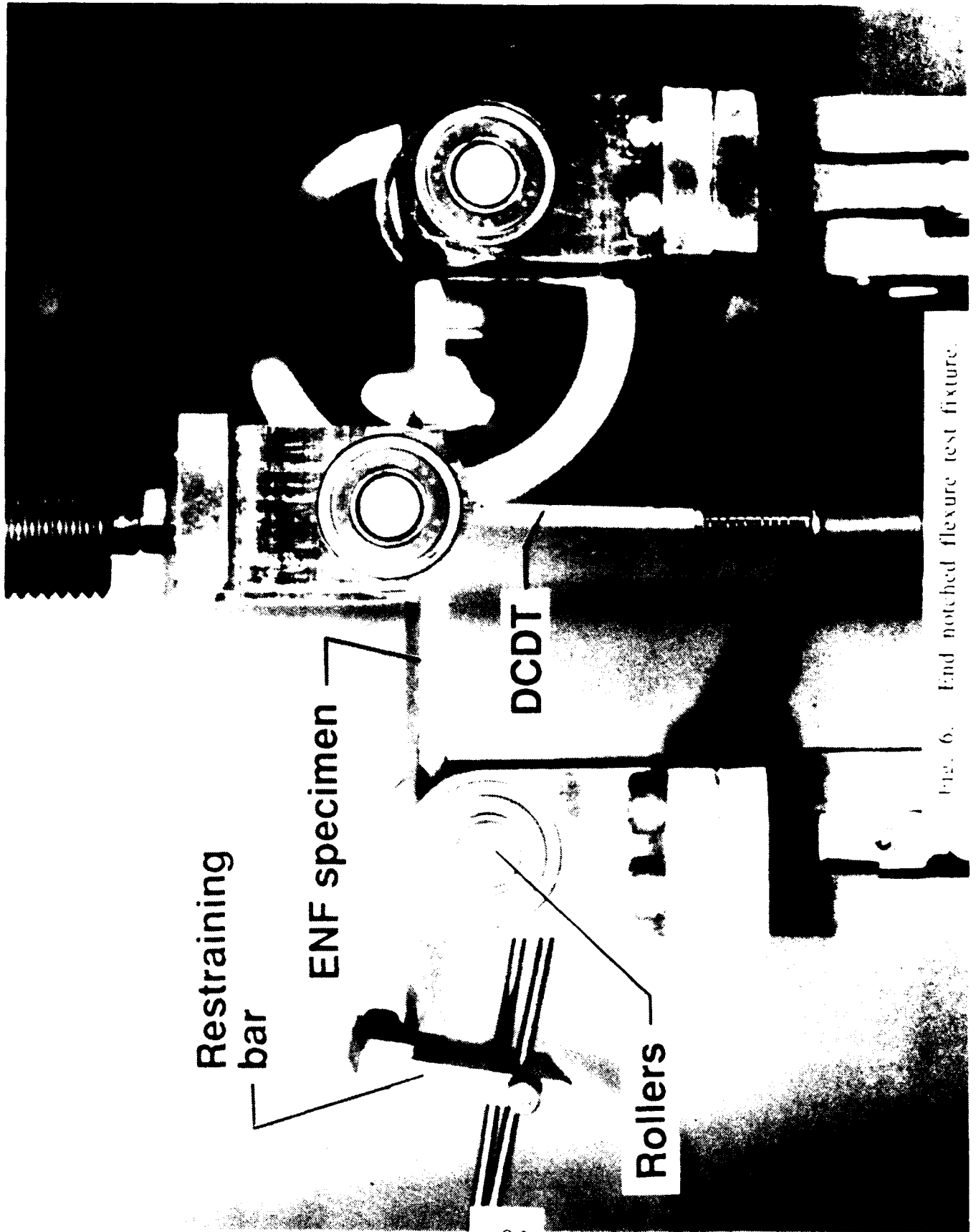


Fig. 6. End notched flexure test fixture.

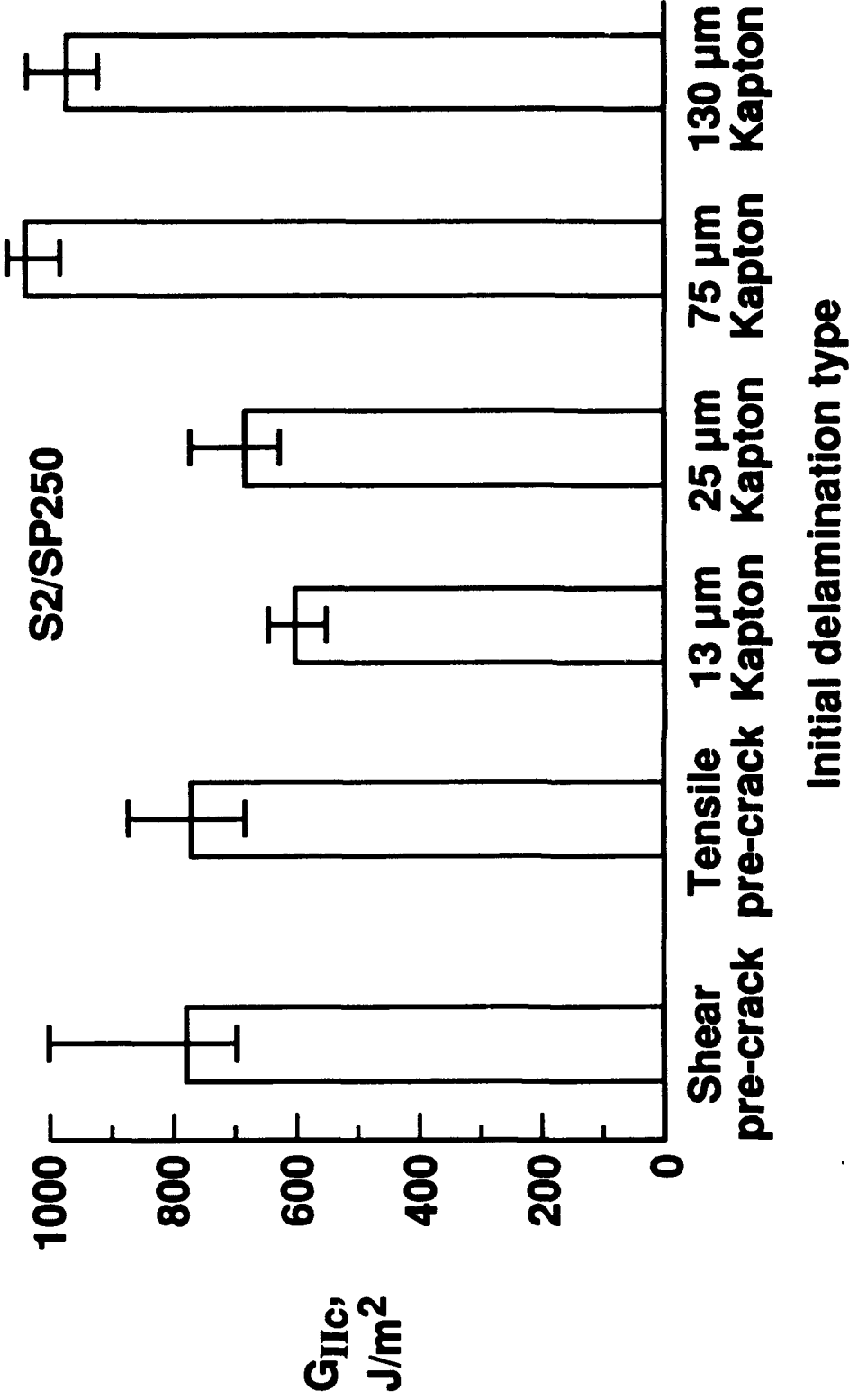


Fig. 7. - Effect of initial delamination on  $G_{IIc}$  at initiation.

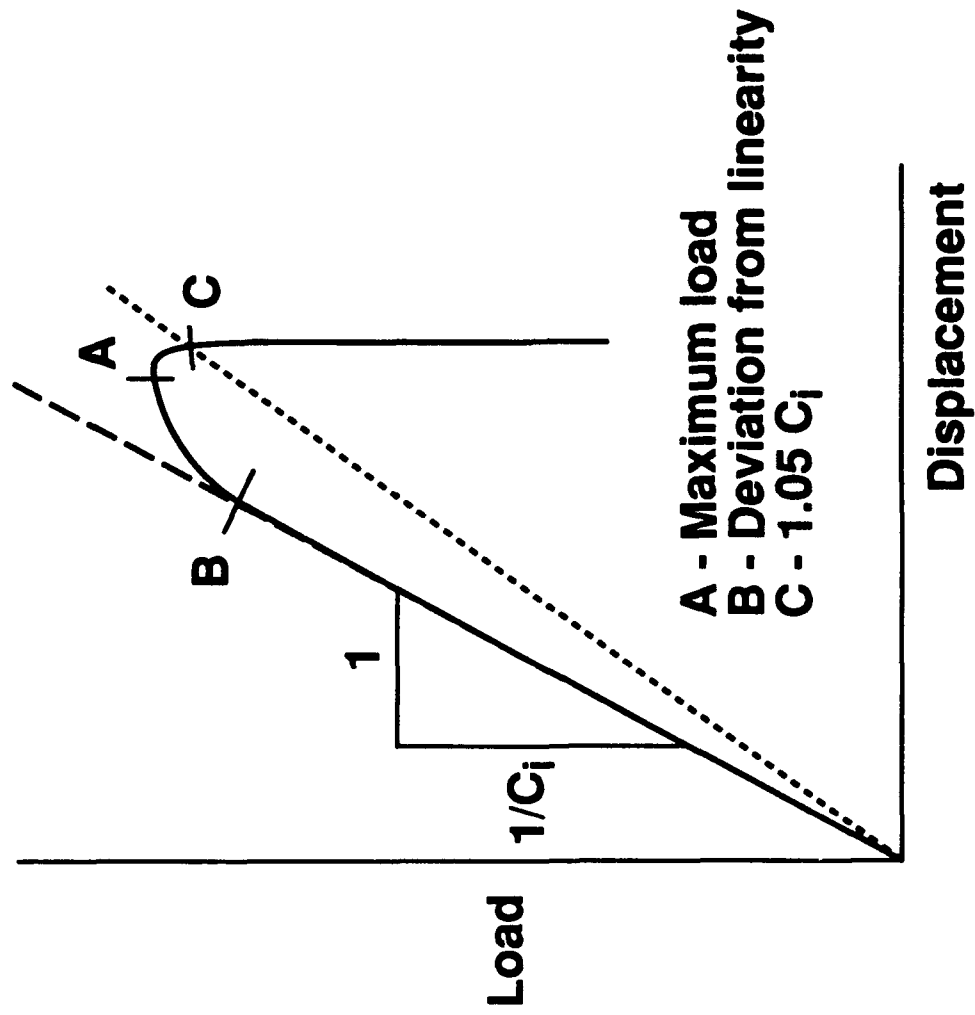


Fig. 8. - Schematic of load-displacement plot for ENF specimen.

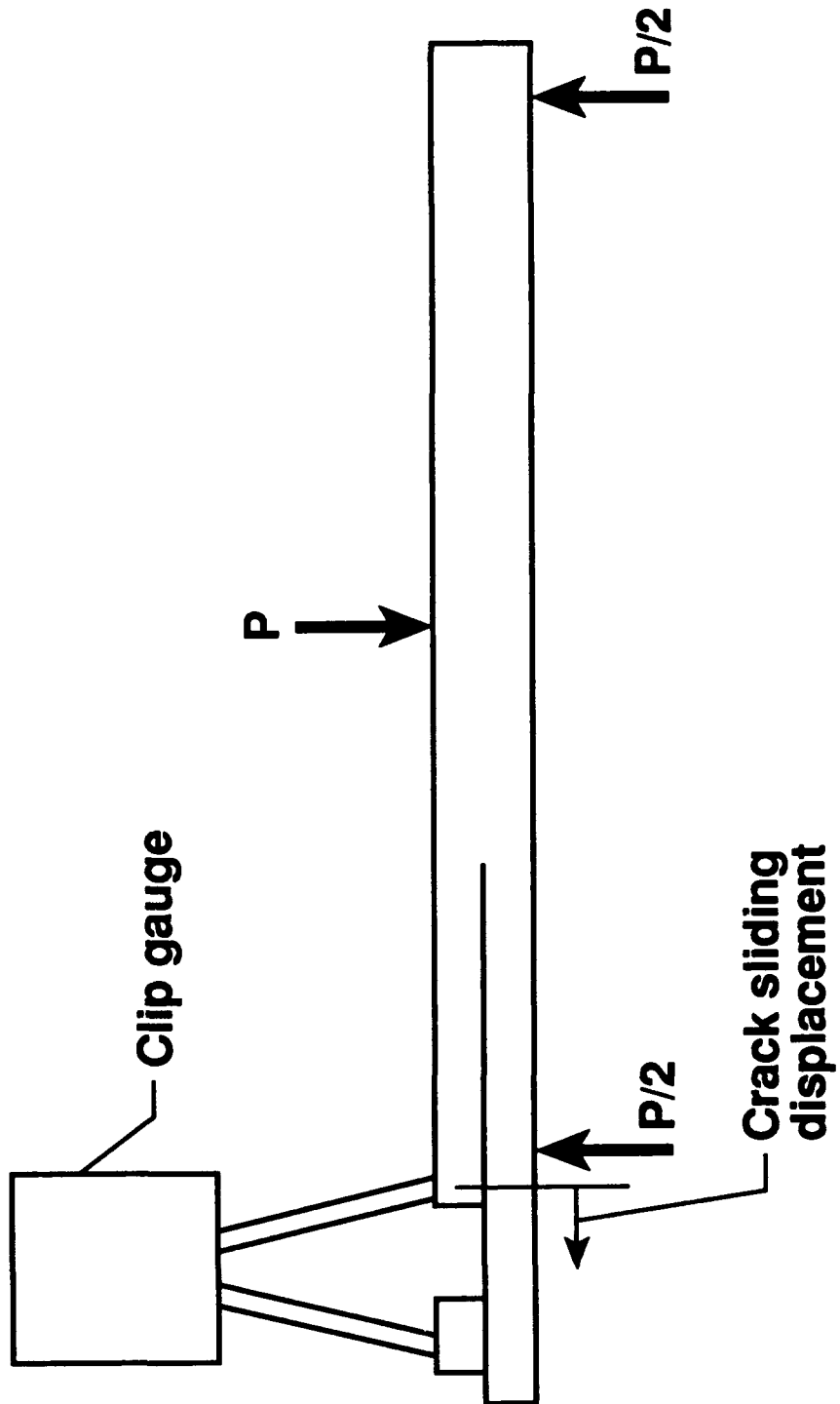


Fig. 9. - ENF specimen controlled by crack sliding displacement.

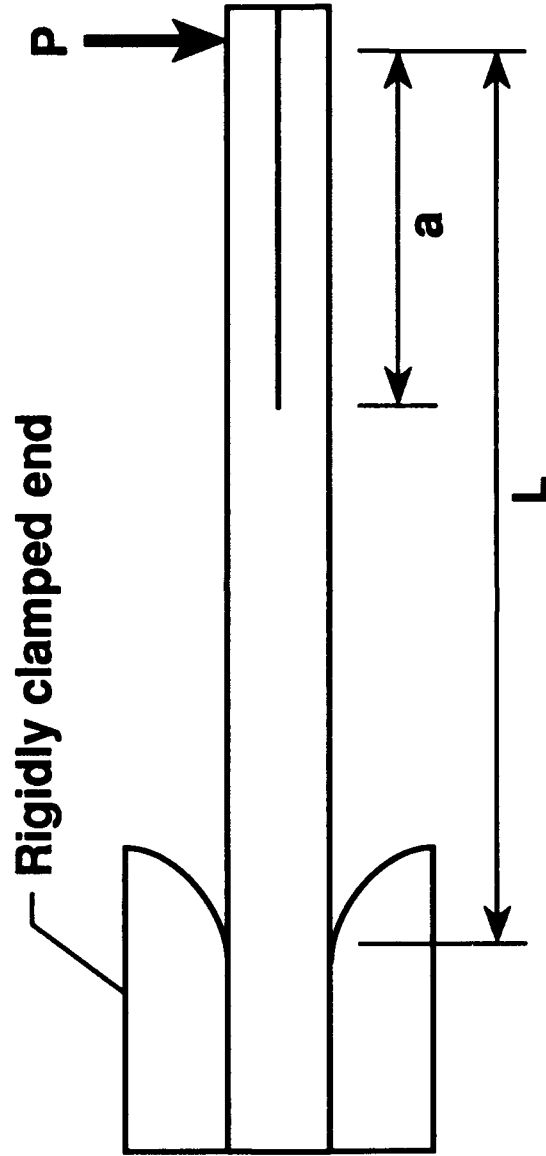


Fig. 10. - Schematic of end loaded split specimen.

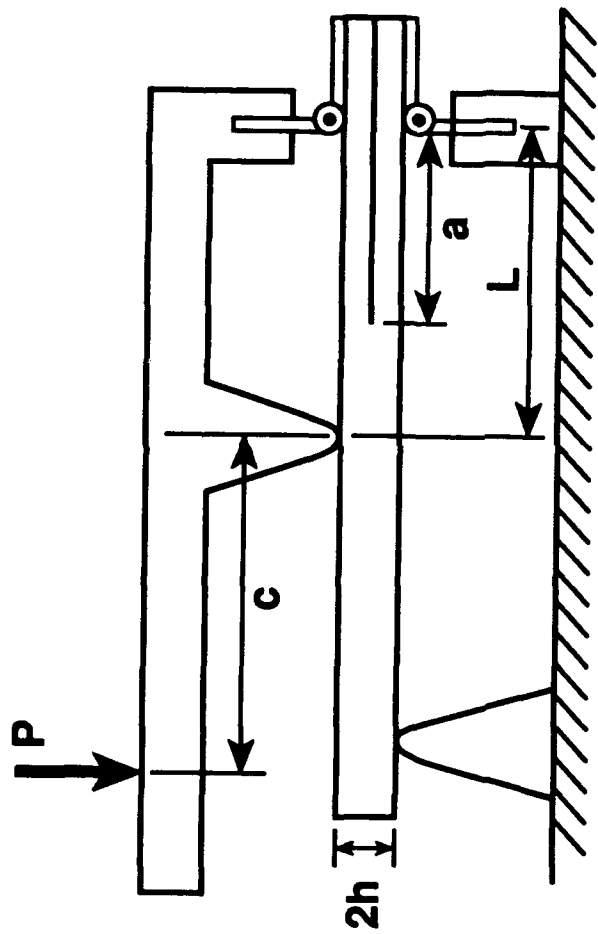


Fig. 11. - Schematic of the mixed mode bend specimen.

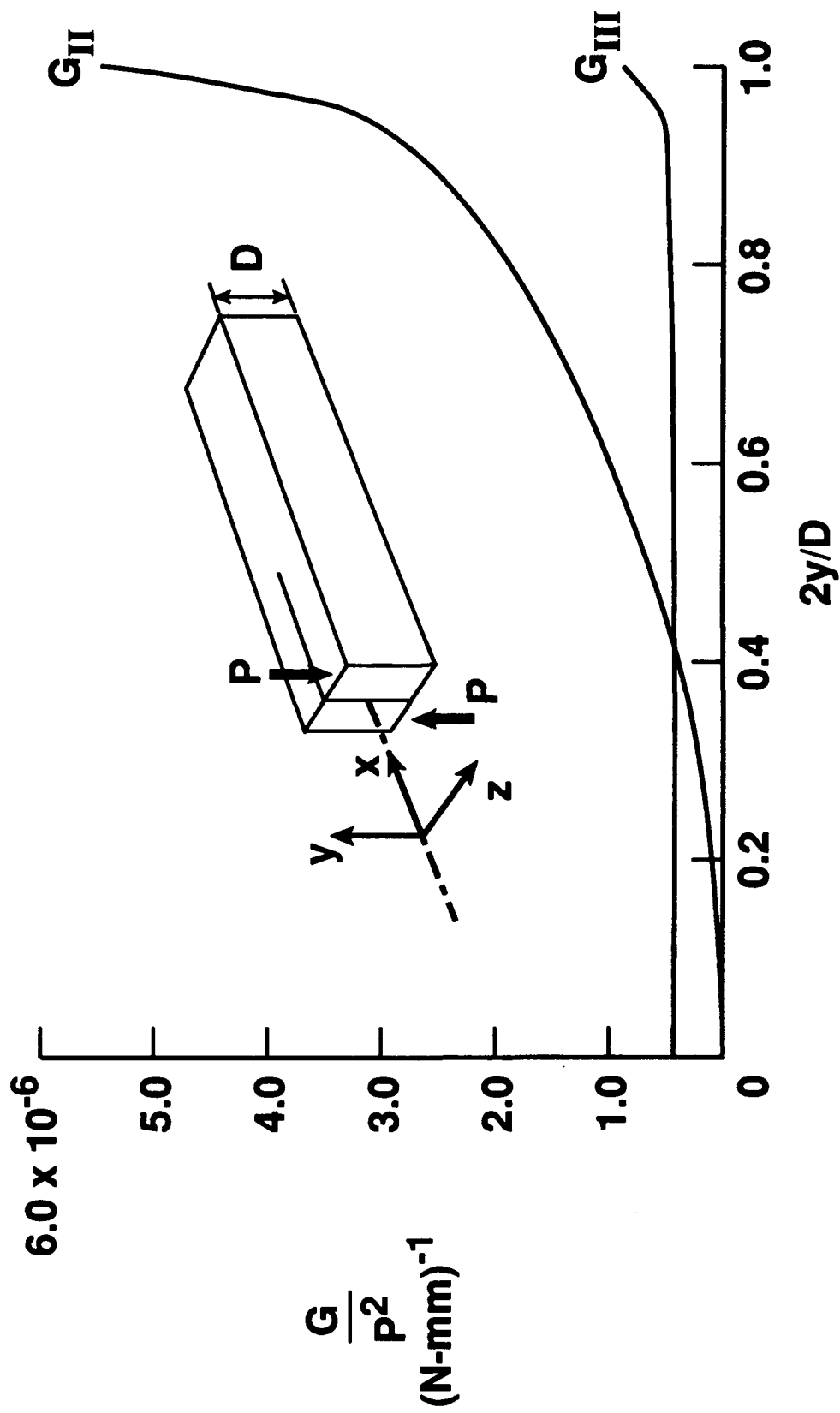


Fig. 12. -  $G_{II}$  and  $G_{III}$  distribution along delamination front.

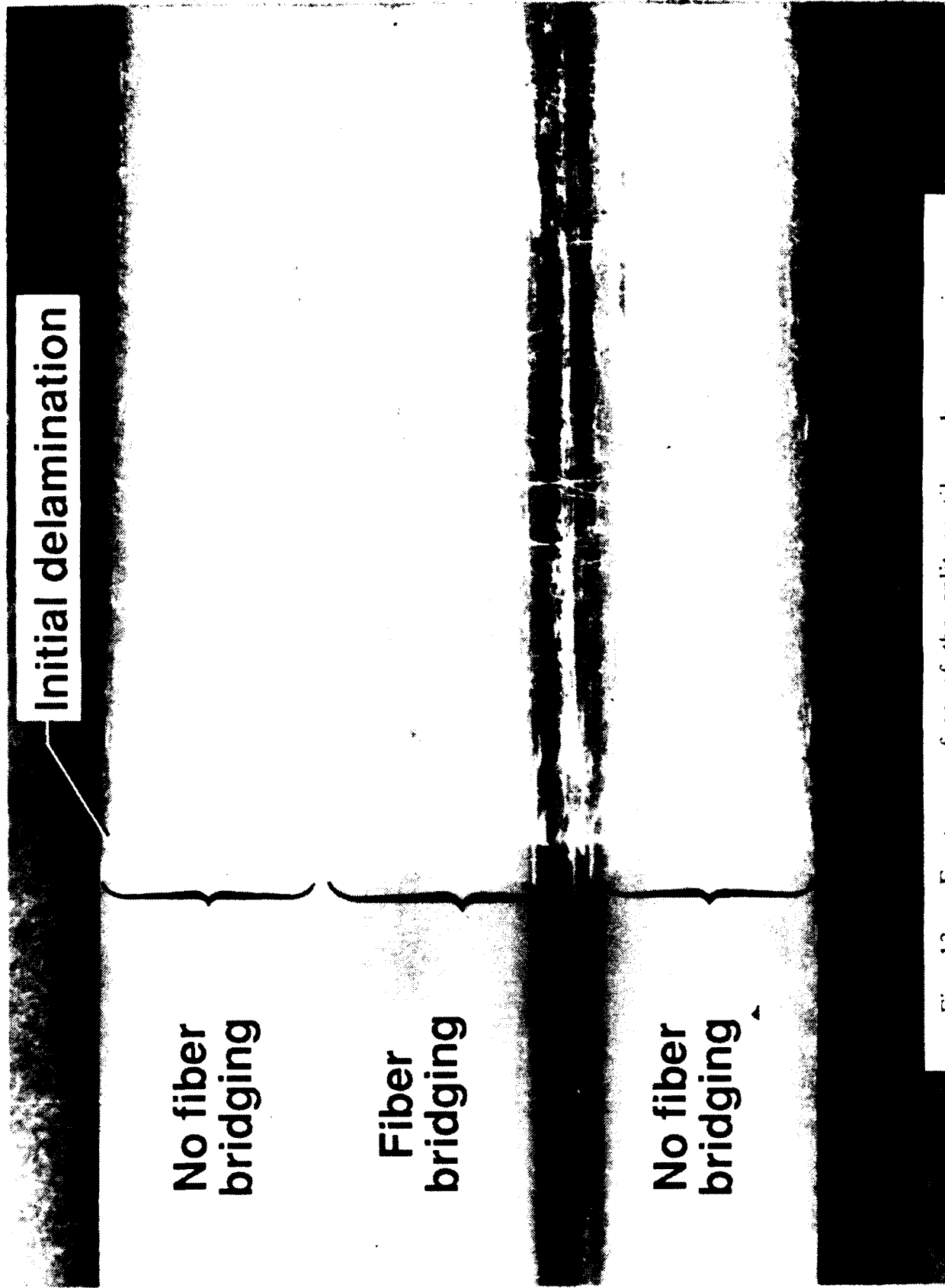
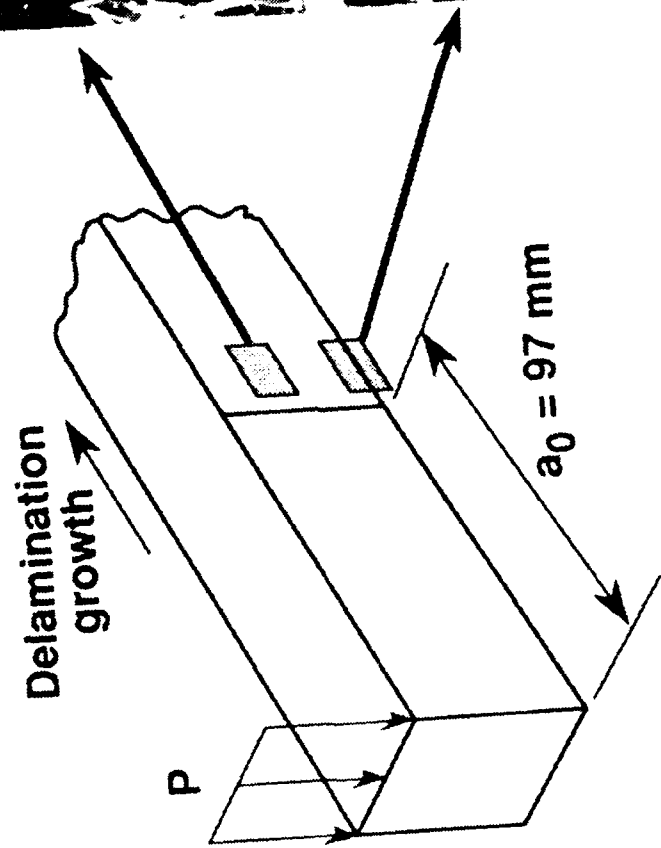
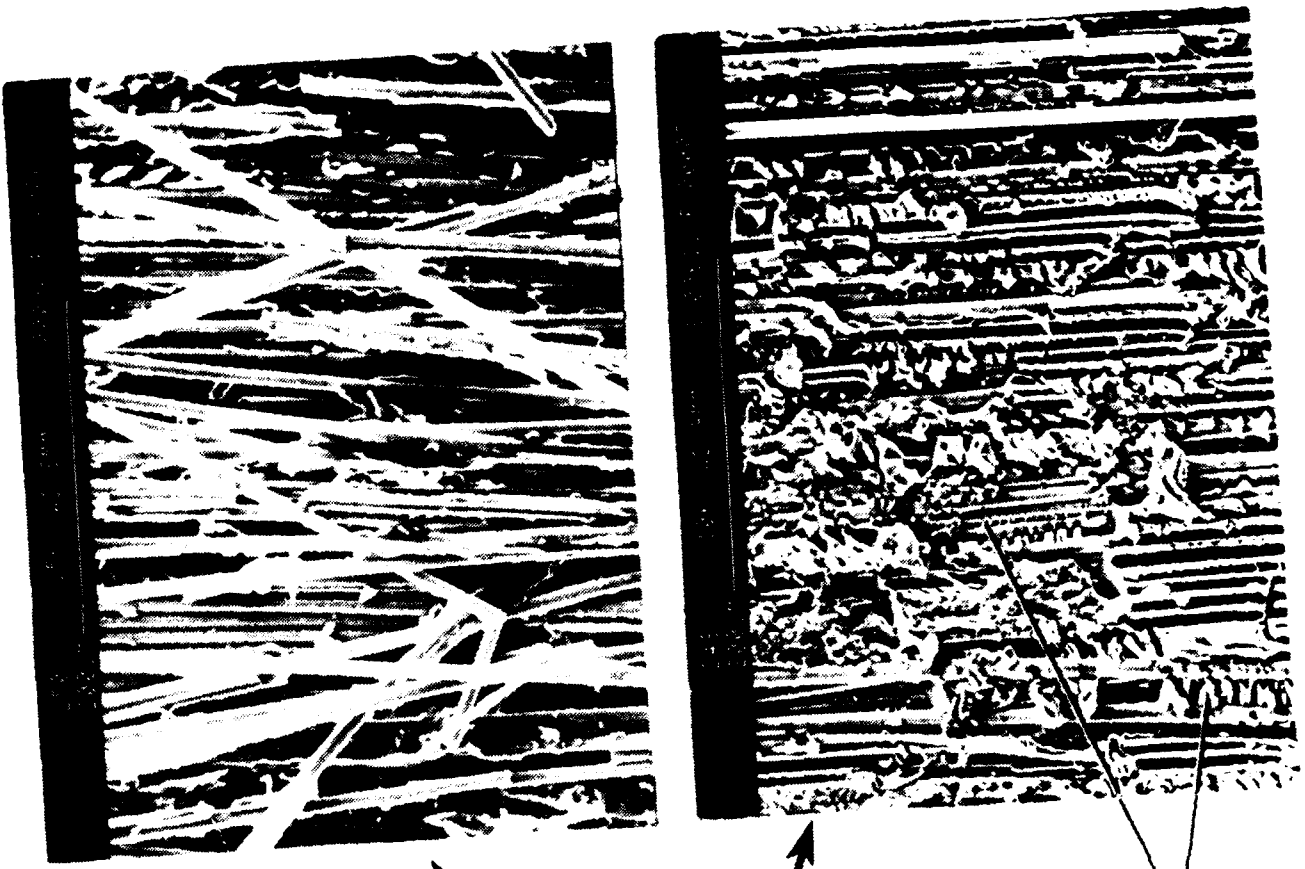
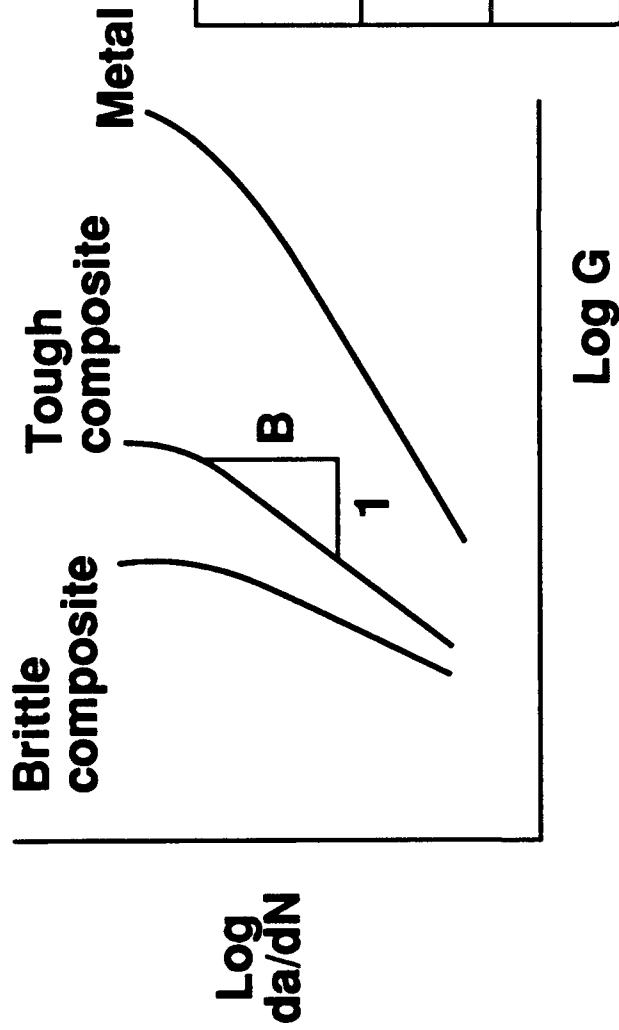


Fig. 13. - Fracture surface of the split cantilever beam specimen.



Mode II shear hackles

Fig. 14. - Micrographs of the fracture surface on the split cantilever beam specimen.



$$da/dN = AG^B \quad G \propto P^2 \Rightarrow da/dN \propto P^{2B}$$

| Materials                 | B    |
|---------------------------|------|
| BS4360 steel              | 1.6  |
| 2024 aluminum alloy       | 2.2  |
| AS4/PEEK gr/thermoplastic | 6.1  |
| S2/SP250 glass/epoxy      | 12.2 |

Fig. 15. - Schematic of delamination growth characterization.

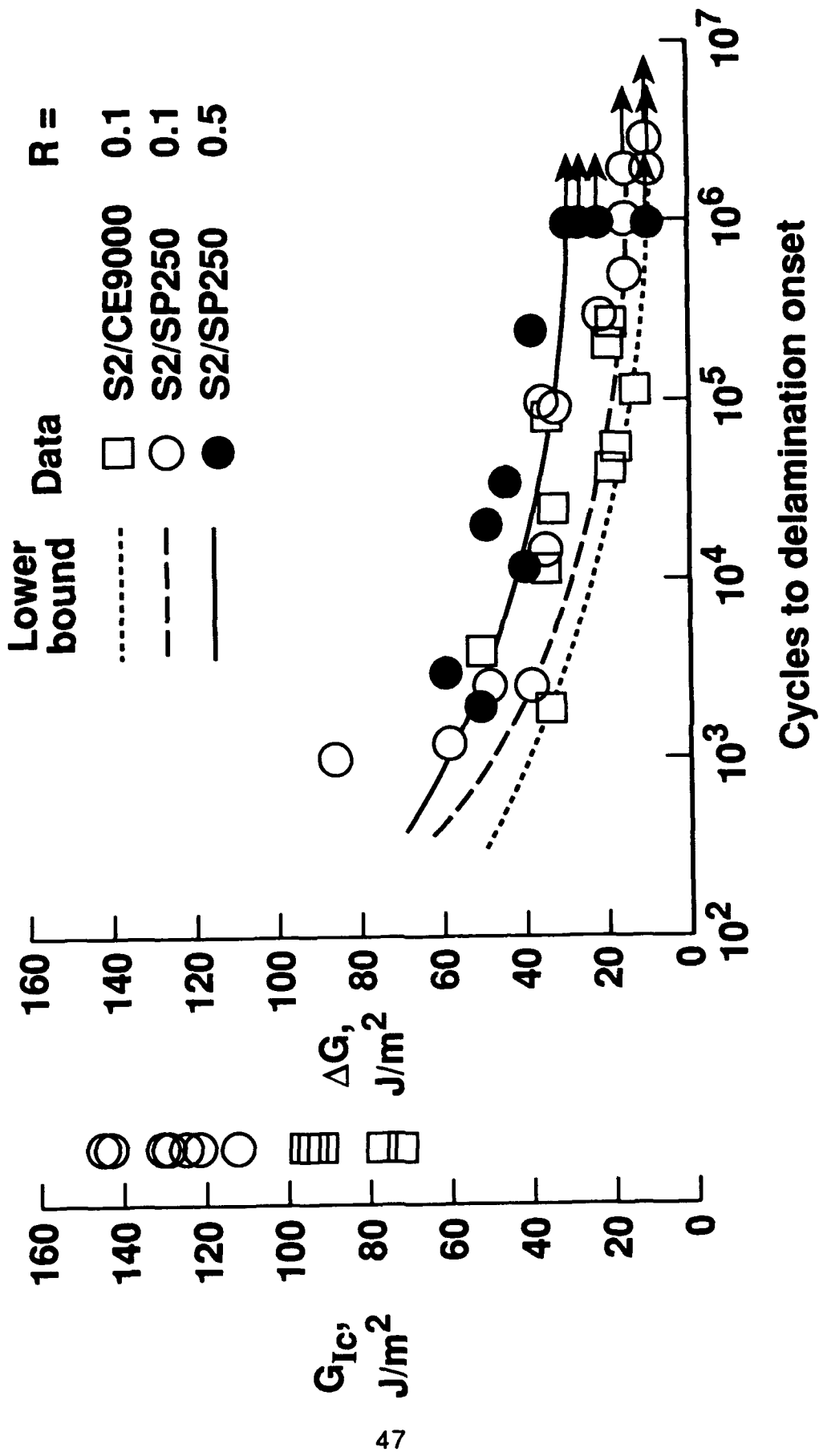


Fig. 16. - Delamination onset data for S2/SP250 and S2/CE9000 composites.

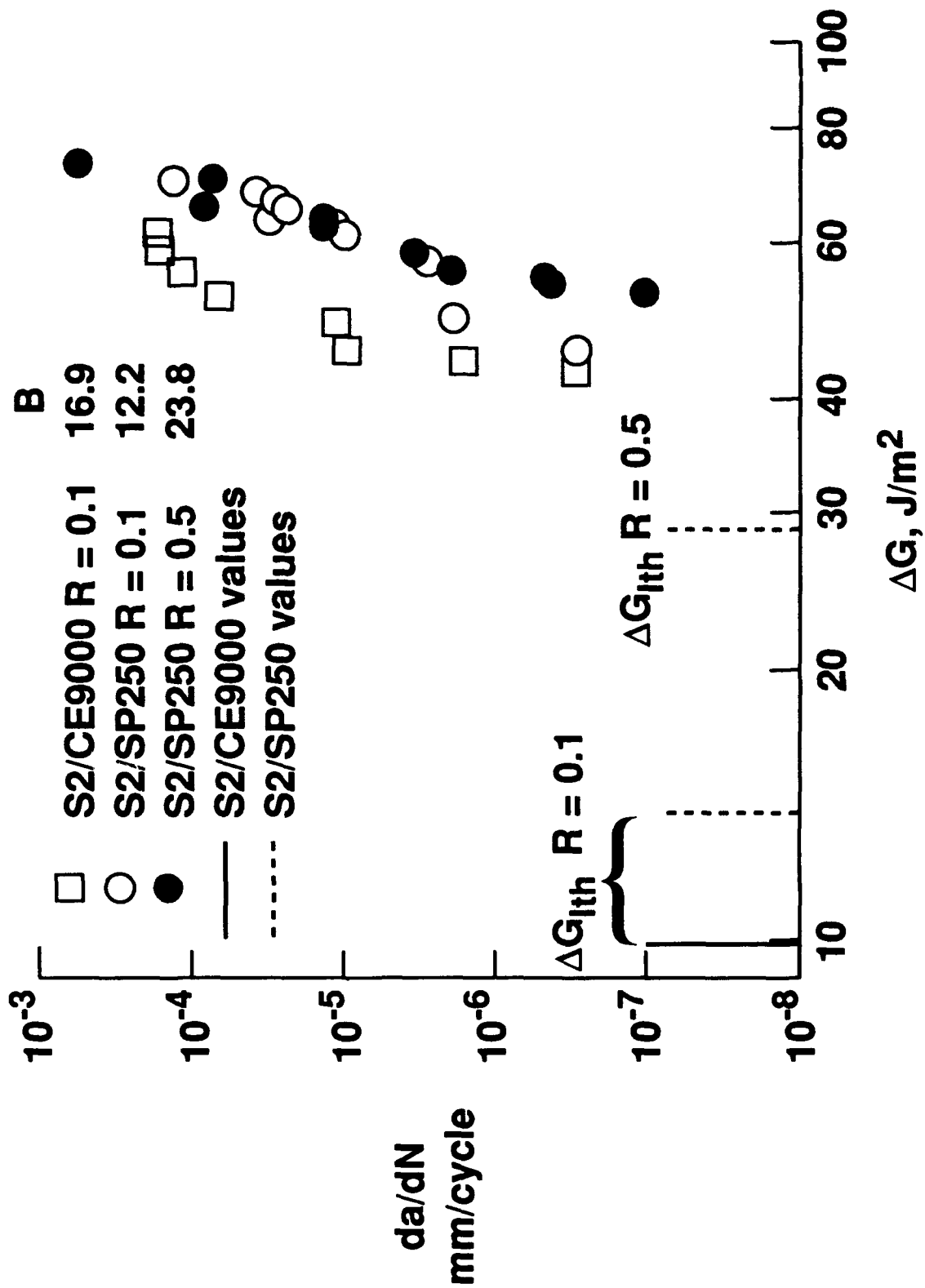


Fig. 17. - Delamination growth data for S2/SP250 and S2/CE9000 composites.



# Report Documentation Page

|  |  |   |  |                               |                         |
|--|--|---|--|-------------------------------|-------------------------|
| 1. Report No.<br><b>NASA CR-187573</b>   |  | 2. Government Accession No.                                 |  | 3. Recipient's Catalog No.    |                         |
| 4. Title and Subtitle<br><b>Interlaminar Fracture Characterization:<br/>A Current Review</b>   |  |   | 5. Report Date<br><b>July 1991</b>   |                               |                         |
|  |  |   | 6. Performing Organization Code  |                               |                         |
| 7. Author(s)<br><b>Roderick H. Martin</b>  |  |   | 8. Performing Organization Report No.  |                               |                         |
|  |  |   | 10. Work Unit No.<br><b>505-63-50-04</b>   |                               |                         |
| 9. Performing Organization Name and Address<br><b>Analytical Services &amp; Materials, Inc.<br/>107 Research Drive<br/>Hampton, VA 23666</b>   |  |   | 11. Contract or Grant No.<br><b>NAS1-18599</b>   |                               |                         |
|  |  |   | 13. Type of Report and Period Covered<br><b>Contractor Report</b>  |                               |                         |
| 12. Sponsoring Agency Name and Address<br><b>National Aeronautics and Space Administration<br/>Langley Research Center<br/>Hampton, VA 23665-5225</b>  |  |   | 14. Sponsoring Agency Code   |                               |                         |
|  |  |   | 15. Supplementary Notes<br><br><b>Langley Technical Monitor: Charles E. Harris<br/>Abridged version of paper to be presented at the 2nd Japan International SAMPE Symposium,<br/>Nippon Convention Center, Tokyo, Japan, December 11-14, 1991.</b> |                               |                         |
| 16. Abstract<br><br><b>Interlaminar fracture characterization has been investigated for several years. Only now is it well enough understood for standardization organizations to attempt to write standard test methods. This paper gives a review of the current philosophies in characterizing interlaminar fracture. The paper covers all modes of interlaminar fracture for brittle and ductile composites. First, the mode I, double cantilever beam test (DCB) for measuring <math>G_{Ic}</math> and the end notched flexure test (ENF) for measuring <math>G_{IIc}</math> are discussed. These tests have undergone the most extensive research throughout the years and are furthest towards standardization. In addition, the mode II, end loaded split (ELS) specimen is discussed. Mixed mode fracture is also discussed and the recently developed mixed mode bending (MMB) test is detailed. Then tests for evaluating mode III fracture toughness, including the split cantilever beam (SCB), are reviewed. Last, the work done on interlaminar fracture characterization in fatigue is reviewed.</b> |  |   |  |                               |                         |
| 17. Key Words (Suggested by Author(s))<br><b>End Notched Flexure<br/>Composite materials<br/>Double Cantilever Beam<br/>Delamination<br/>Strain energy release rate</b>  |  |   | 18. Distribution Statement<br><br><b>Unclassified - Unlimited<br/>Subject Category - 39</b>  |                               |                         |
| 19. Security Classif. (of this report)<br><b>Unclassified</b>  |  | 20. Security Classif. (of this page)<br><b>Unclassified</b> |  | 21. No. of pages<br><b>49</b> | 22. Price<br><b>A03</b> |